

Chapter 7

Automated Determination of Complex Surface Structures by LEED

M.A. Van Hove

*Center for Advanced Materials, Materials Sciences Division, Lawrence Berkeley Laboratory,
Berkeley, CA 94720, USA*

and

Department of Chemistry, University of California, Berkeley, CA 94720, USA

W. Moritz

*Institut für Kristallographie und Mineralogie, Universität München, Theresienstrasse 41, 8000
München 2, Germany*

H. Over

Fritz-Haber-Institut der Max-Planck-Gesellschaft, Faradayweg 4–6, 1000 Berlin 33, Germany

P.J. Rous

Department of Physics, University of Maryland Baltimore County, Catonsville, MD 21228, USA

A. Wander

*Department of Physical Chemistry, University of Cambridge, Lensfield Road, Cambridge CB2
1EW, UK*

A. Barbieri, N. Materer, U. Starke and G.A. Somorjai

*Center for Advanced Materials, Materials Sciences Division, Lawrence Berkeley Laboratory,
Berkeley, CA 94720, USA*

and

Department of Chemistry, University of California, Berkeley, CA 94720, USA

Contents

1. The challenges of structural complexity	194
1.1. Limits of conventional LEED crystallography	194
1.2. Automation of LEED crystallography	195
1.3. Types of structural complexity	196
1.4. Topics of discussion	196
2. Lessons from X-ray crystallography	197
2.1. Initial structural guesses	197
2.2. XRD more accurate than LEED	197
2.3. Database size	198
2.4. Least-squares refinement	198
2.5. Estimating the reliability of the result	199
2.6. Implications for LEED	199
3. Efficient LEED calculations	199
3.1. Tensor-LEED theory	200
3.1.1. Concepts	200
3.1.2. Linear tensor LEED	201
3.1.3. Tensor LEED	201
3.1.4. Accuracy of TLEED	202
3.1.5. Efficiency of TLEED	202
3.1.6. Applications	203
3.2. Nonlinear least-squares fit	203
3.2.1. Concepts	203
3.2.2. Calculating derivatives	203
3.2.3. Applications	205
3.3. Linear LEED	206
3.3.1. Concepts	206
3.3.2. Accuracy of LLEED	209
3.3.3. Potential applications	209
4. Search algorithms	210
4.1. Types of search methods	210
4.2. Direct methods in LEED	210
4.3. Marquardt approach	211
4.4. Simplex method	212
4.5. Direction-set method	213
4.6. Rosenbrook method	213
4.7. Hooke–Jeeves method	213
5. Practical issues	213
5.1. Achievable level of automation	214
5.2. Required quality of LEED theory	214
5.2.1. Quick and rough searches	214
5.2.2. Lattice parameters	215
5.2.3. Atomic scattering amplitude	215
5.2.4. Relative importance of non-structural parameters	216
5.2.5. Muffin-tin zero	216
5.2.6. Damping	216
5.2.7. Thermal vibrations	217
5.2.8. Optimizing non-structural parameters	217
5.3. Required experimental database	218
5.3.1. I - V -curve smoothing	218
5.3.2. Database size	218

5.3.3. Off-normal incidence	219
5.3.4. Use of subsets of data	219
5.4. <i>R</i> -factors	219
5.4.1. <i>R</i> -factor definitions	219
5.4.2. Using multiple <i>R</i> -factors	221
5.4.3. Clusters of <i>R</i> -factor minima	221
5.4.4. Avoiding fine-scale roughness of <i>R</i> -factors	221
5.4.5. Sensitivity to experimental errors	221
5.4.6. Theoretical energy steps	222
5.4.7. Required number of <i>R</i> -factor evaluations	222
5.5. Optimization strategies	223
5.5.1. Optimizing subsets of parameters	223
5.5.2. Iterating the search	224
5.5.3. Checking for a minimum	224
5.6. Structural precision and accuracy	224
5.6.1. Accuracy poorly known	224
5.6.2. Estimating error bars	225
5.6.3. Correlated parameters	225
5.6.4. Error bar definitions	225
5.6.5. Examples	226
6. Applications to other spectroscopies	226
7. Conclusions and outlook	226
Acknowledgments	227
References	227

Automated determination of complex surface structures by LEED

M.A. Van Hove^a, W. Moritz^b, H. Over^c, P.J. Rous^d, A. Wander^e,
A. Barbieri^a, N. Materer^a, U. Starke^a and G.A. Somorjai^a

^a Center for Advanced Materials, Materials Sciences Division, Lawrence Berkeley Laboratory, Berkeley,
CA 94720, USA

and

^b Department of Chemistry, University of California, Berkeley, CA 94720, USA

^b Institut für Kristallographie und Mineralogie, Universität München, Theresienstrasse 41,
8000 München 2, Germany

^c Fritz-Haber-Institut der Max-Planck-Gesellschaft, Faradayweg 4–6, 1000 Berlin 33, Germany

^d Department of Physics, University of Maryland Baltimore County, Catonsville, MD 21228, USA

^e Department of Physical Chemistry, University of Cambridge, Lensfield Road, Cambridge CB2 1EW, UK

Conventional surface crystallography by low-energy electron diffraction (LEED) employs a trial-and-error search controlled at each step by human effort. This trial-and-error approach becomes very cumbersome and unreliable to solve complex surfaces with a large number of unknown structural parameters. We discuss automatic optimization procedures for LEED, which combine numerical search algorithms with efficient methods of determining the diffracted intensities for varying structures. Such approaches can reduce the computer time required for an entire structure determination by many orders of magnitude, while fitting many times more unknown structural parameters. Thereby, relatively complex structures, with typically 10 adjustable atoms (or 30 adjustable coordinates), can be readily determined on today's workstations. These include non-symmetrically relaxed structures, surface reconstructions and adsorbate-induced substrate distortions. We also address the theoretical and experimental requirements for an accurate structural determination.

1. The challenges of structural complexity

1.1. Limits of conventional LEED crystallography

Until recently, the application of the technique of low-energy electron diffraction (LEED) [1–3] has been confronted by a theoretical barrier which has largely prevented the determination of many complex surface structures. This barrier is due to the presence of many independent atoms in the surface unit cell [4,5] combined with the extensive computational requirements of multiple scattering, as expressed in the dynamical theory of LEED. In addition, the traditional approach to the determination of surface structure with LEED demands large computing times and cumbersome trial-and-error searches for optimal parameters which define the “best-fit” structure.

The most apparent limitation of LEED is the way in which the time taken to perform a single calculation of LEED-intensity spectra scales with the number of inequivalent atoms in the surface unit cell. The N^3 , or at best N^2 , scaling behavior reflects the nature of the multiple-scattering problem which, in simplest terms, requires the summation of all multiple-

scattering paths between the N non-equivalent atoms in the surface. Over the past two decades, most theoretical advances in LEED have been aimed at reducing the computational resources needed for a single LEED calculation. This problem has been successfully addressed by a number of approximations to full multiple scattering, which, by the neglect of certain contributions to the scattered intensity, increase the efficiency of a LEED calculation. Examples are renormalized forward scattering [1], reverse-scattering perturbation [6], quasi-dynamical LEED [7–9] and the beam-set-neglect method [4,10]. Also, a large gain in the speed of the computation can be obtained by using symmetry-adapted functions in the angular-momentum expansion [11–13].

However, the LEED calculation has primarily been used within the context of a structure determination in which $I-V$ spectra are repeatedly computed in order to find the best-fit surface structure. Thus, the less apparent, but in many ways more serious, limitation of LEED arises from the traditional trial-and-error method of determining a surface structure, in which human selection of new trial structures is required. This procedure also compares the experimental intensity spectra ($I-V$ curves) to the results of LEED calculations for a series of trial structures, with the help of R -factors that measure the misfit between theory and experiment. The time taken to perform this trial-and-error search scales exponentially with the number of varied parameters. For example, if one wishes to determine three structural parameters, one must exhaustively explore all corners of a cubic parameter space. The prospects for reliably determining in this manner the best-fit structure when fitting tens of parameters are clearly limited: most likely, significant regions of such a large volume of parameter space will remain unexplored.

1.2. Automation of LEED crystallography

Structural complexity demands a more sophisticated approach to the structure search, one in which the refinement of the model surface structure proceeds in an automated and organized manner. Indeed, the concept of using a directed search through parameter space has been suggested since the beginning of quantitative LEED structure determinations [3,14]. Of course, such a search is commonly used in X-ray crystallography [15]. Therefore, in the last 6 years or so, the focus of theoretical developments in LEED has been the adaptation of dynamical-LEED theory to the requirements of directed structural searches [16–20]. The recent achievements promise automation of surface structures by LEED for the near future. However, one must not expect push-button, hands-off automation: as in X-ray crystallography, various models must be tried and results verified with a series of separate searches, chosen by a human being rather than by a computer.

One drawback of incorporating a search method into full dynamical LEED is that one is forced to abandon an efficient feature used in such calculations [18]. Conventional LEED greatly benefits from the multiple re-use of costly energy-dependent quantities for many trial structures, before moving on to the next energy; only after all desired energies have been processed can a comparison be made with experiment for all those trial structures. By contrast, an automated search strategy needs the diffracted intensities at all energies for only one trial structure at a time. Thus, by attempting to increase the efficiency of the structure determination by using a directed search, the efficiency of the calculation of $I-V$ spectra for each trial structure is reduced, unless other measures are taken. (This difficulty can be partially overcome with modern workstations and supercomputers with a large memory that allows the storage of the layer-diffraction matrices for all energies.) This state of affairs is the

result of multiple scattering, which differentiates LEED markedly from X-ray diffraction in terms of computational requirements.

1.3. Types of structural complexity

There are various types of structural complexity that one must envisage: the theoretical methods that will most efficiently yield the solution will depend on the type of complexity involved. Conventional LEED theory is most efficient for structures which have only one atom in the two-dimensional surface unit cell per layer, provided that these layers are well separated (by at least about 0.7 Å, more often about 1.0 Å). This applies to many common unreconstructed clean-crystal terminations, like the (111), (100) and (110) faces of fcc metals, the (110) and (100) faces of bcc metals and the (0001) face of hcp metals, but very few other clean surfaces. Atomic adsorption on these “low-Miller-index” surfaces also often yields a simple structure, if one neglects lateral relaxations induced in the substrate.

Most surfaces of technological interest are not so simple. Semiconductors, whether clean or adsorbate-covered, usually reconstruct with large relaxations from the bulk lattice that extend many layers below the surface. Compounds (from metallic to covalent to ionic) often reconstruct or relax in complex ways. On metals, adsorbates can induce small (~ 0.1 Å), but significant local relaxations that are also complex, or can even cause larger-scale reconstructions of the substrate. More complex adsorbates, like molecules, also present many unknown coordinates to be determined, as the adsorbate distorts under the influence of the bonding to the substrate, and vice versa. For these various types of complex surface, new methods have now proven their ability to yield detailed structure determinations very efficiently and almost automatically. This review will concentrate on these developments.

Adsorbates on substrates may also be disordered. The same complexities of mutually induced relaxations or reconstructions can occur in the disordered case as well. Some of the efficient methods of structural solution which we shall describe for ordered structures are easily applied also to such disordered overlayers [21,22].

Stepped surfaces (i.e. surfaces which have high Miller indices) have always presented difficulties for LEED theory even with the conventional trial-and-error methods. Progress has been achieved to enable the calculation of LEED intensities for a given stepped structure with or without relaxations and adsorbates [23–26]. Here again, some of the new efficient methods to be described for solving complex ordered structures can be added to the stepped-surface analysis, thereby allowing their efficient determination [25,26].

Other forms of structural complexity have not yet received much attention. One such case is incommensurate lattices, which occur frequently in hetero-epitaxy and in weak adsorption. The incommensurability translates into non-periodic local relaxations that are at present difficult to extract from experiment. Another form of complexity is provided by polymers and biopolymers, so far largely unexplored. Yet another is the structure of amorphous or liquid surfaces, where so far virtually no structure determination of any sort has been possible with LEED.

1.4. Topics of discussion

The fundamental difficulty in optimizing many structural parameters is their correlation through diffraction: one cannot fit one parameter at a time, but has to fit them all simultaneously, since diffraction inevitably couples them together. Therefore, given a set of experimental I - V curves, the problem of structure determination by LEED has three

requirements. Firstly, one needs a means of calculating as efficiently as possible diffracted intensities at each step in the search. Secondly, one needs a strategy for searching through parameter space to efficiently locate the best-fit structure. Finally, one needs a means of comparing the calculated intensities to the measured spectra which serves as our guide for continuing the structure search.

Below, we review and discuss recent progress in implementing efficient methods of determining complex structures with LEED. These methods promise automation of surface crystallography in the near future. First, in section 2, we shall draw lessons from the long and successful practice of X-ray crystallography. Then, in section 3, our attention will focus on the various methods that have been applied so far to increase the efficiency of the LEED computations for single structures and for modified structures related to another one: these include tensor LEED, linear expansions and linear LEED. We shall next address, in section 4, optimization algorithms that have proved fruitful for LEED, such as direct methods, least-squares fitting, and the Rosenbrook, direction-set and simplex methods. Importantly, we shall discuss in section 5 implications for practical surface crystallography by LEED, based on the experience gained in the recent past. It will be stressed, in section 6, that the methods developed for LEED are also applicable to other techniques of surface-structure determination, such as photoelectron and Auger electron diffraction, and high-resolution electron energy-loss spectroscopy. Finally, we shall conclude and look at future prospects in section 7.

2. Lessons from X-ray crystallography

2.1. Initial structural guesses

The long and successful practice of X-ray crystallography contains very useful lessons for the 50-years younger field of LEED crystallography. Since both methods are diffraction techniques, the problems and limitations of crystallography are in principle the same. The main difference lies in the way a suitable initial structural model is found. With X-ray diffraction (XRD), a number of methods are available to arrive at an approximate guess of the structure more or less directly from the experimental data (e.g. the Patterson function and Fourier synthesis). There are also so-called direct methods which allow a structure determination directly from the intensities for structures of limited complexity (routinely up to about 80 independent atoms at present); so far, no suitable equivalent method has been introduced in the case of LEED, where a good initial guess of the structure is required (even in the case of the “direct methods” of LEED). As far as the structure refinement is concerned (i.e. final optimization of parameters starting from a good initial structure) both methods should be comparable. Nevertheless, some differences exist here as well, and that will be the focus of the following discussion.

2.2. XRD more accurate than LEED

Compared with X-ray diffraction, the calculation of LEED intensities is much more complicated, the theory uses additional approximations and has additional non-structural parameters: spherical atomic potentials, constant inner potential (muffin-tin zero), neglect of the potential barrier at the surface, uniform absorption and isotropic temperature factors [1,3]. We therefore cannot expect the structural results obtained from LEED to be more precise than those determined with X-rays, nor can we expect that refinement techniques

work better than with X-rays. A brief summary of the structure-refinement techniques of XRD therefore will exhibit the best-case limits for LEED.

2.3. Database size

For XRD the number of (symmetrically inequivalent) measured beam intensities is typically a factor of 5–10 larger than the number of free parameters to be fit. Smaller redundancies are frequently used if more data cannot be measured or if the data are very precise. The accuracy which can be obtained for the interatomic distances is in most cases not larger than 0.01 Å. Nevertheless, the standard deviation usually quoted for the positional parameters is often much smaller than this (e.g. 0.001 Å), but it is calculated assuming statistical errors and a certain model for thermal vibrations, neglecting systematic errors. Note, on the other hand, that the lattice parameters (lattice constants) can be determined with much higher precision than this (unlike in LEED, where bulk substrate values from XRD are usually assumed without check).

In the case of LEED the data redundancy must be viewed in the context of continuous curves rather than individual data points: continuous curves of intensity as function of energy (or angles). With many angles of incidence and large energy ranges, the data base is in principle much larger than in the case of X-rays. However, frequently only the data at normal incidence are used and the database then becomes comparable to the situation with X-rays. In the case of LEED I - V curves (intensity versus energy curves), the number of independent data points is often estimated to be equal to the number of measured maxima. (It should be kept in mind that the I - V curves can be approximated as a superposition of Lorentzian curves of similar width [27].) If we assume an average peak separation of about 15 eV, the independent information in the I - V curves with a total range of 3000 eV amounts to about 200 data points. The free parameters to be fit to experiment are primarily the structural parameters, the inner potential and the thermal vibrations. The scale factors, which are needed for each beam independently to compare experimental and theoretical intensities, have to be taken as free parameters as well. In the above mentioned case, which might correspond to, say, 15 beams and 10 structural and non-structural parameters, this would amount to about 25 free parameters to be determined from 200 data points. This consideration shows us that the redundancy of data is about the same for XRD as for LEED when using normal incidence only.

2.4. Least-squares refinement

The standard method for structure refinement in X-ray analysis is the least-squares optimization using the expansion method [28]. Starting with an arbitrary structure the refinement converges to a local extremum (usually, but not necessarily, a minimum) of the R -factor in the parameter space. It is clear that the starting model must be sufficiently close to the correct structure. How close must it be? A very rough estimate is that the atoms should be within a few tenths of an ångström from the correct positions. If all the atoms are misplaced, it is often not possible to start the full simultaneous refinement of all parameters. One then tries to first refine single parameters or blocks of parameters keeping other parameters fixed, and to proceed stepwise in this way until in the final step all parameters can be freed. For large structures in particular, a block refinement can be used, which however converges more slowly, or constraints can be used to move rigid groups of atoms or molecules in the structure. In any case, one must check that the same minimum is reached when starting with several

different trial structures. The radius of convergence may be larger for single atoms if the major part of the starting model is correct. In general, many cycles of iteration steps are necessary to locate the true minimum of the R -factor.

2.5. Estimating the reliability of the result

In the case of X-rays, the reliability of the result can be checked by the difference Fourier synthesis, which would show missing or misplaced atoms. A comparable technique for LEED has not yet been established as yet and one has to rely on the comparison of the $I-V$ curves and the plausibility of the structure. Besides the R -factor, the main criterion used in XRD to evaluate the quality of the structure analysis is the χ^2 test, which indicates with what probability the mean square deviation lies within the experimental errors. These are obtained from the counting statistics and from comparison of symmetrically equivalent reflections.

2.6. Implications for LEED

From the comparison with X-ray structure analysis, we learn that automatic refinement techniques should be very suitable for LEED, that the standard database size at normal incidence should be sufficient in most cases of current interest, and that one can expect a radius of convergence for the refinement of less than an atomic radius (smaller values are more likely because the LEED intensities depend more strongly on interatomic distances than in the kinematic theory). The relatively large computational effort required to calculate the LEED intensity and its derivatives, however, have led to several different developments to enhance efficiency. (Derivatives of intensities or R -factors are needed by some search algorithms, such as steepest-descent methods and least-squares fitting.)

3. Efficient LEED calculations

This section addresses the very important issue of efficiently evaluating LEED intensities (and their derivatives, if needed) for a single trial structure. These are required to obtain R -factor values (and perhaps R -factor or intensity derivatives) that are used in optimization schemes. The speed of a search is ultimately set by the speed of computing individual LEED intensities.

The choice of method to evaluate LEED intensities must be made in light of the demands of the particular search algorithm used. Optimization algorithms seek to automatically locate the best-fit surface structure, by exploring the R -factor hypersurface in the neighborhood of a trial structure, and by making a sensible guess for an improved trial structure.

Clearly, the tendency toward solving more complex structures with higher accuracy requires that the basic LEED-intensity calculation be as accurate as possible. Therefore, it is not realistic to look for increased computational speed with approximations that degrade the theoretical intensities. However, efficient approximations have been developed to rapidly obtain intensities for structures *closely related* to a "reference structure" for which the intensities have been obtained accurately, and also to obtain derivatives of intensities.

It should be emphasized that the R -factor is not only a function of atomic positions, but also of non-structural parameters, such as the inner potential (more exactly the muffin-tin zero in electron-scattering theory), the phase shifts (i.e. scattering potential), and parameters related to thermal effects and damping. These may also have to be optimized; in fact, the

muffin-tin zero has such a strong influence on structural parameters that it is always treated on an equal footing with them.

Exploring the R -factor hypersurface can be facilitated with derivatives of the R -factor and/or intensities with respect to the parameters to be fit. Due to the complexity of the LEED formalism, it is difficult to obtain explicit expressions for partial derivatives of intensities. And, most R -factors used in LEED being integrals over energy ranges, these have no closed formulas for R -factor partial derivatives. Whenever R -factor partial derivatives are required, they must therefore be obtained numerically from calculations for slightly different parameter values, or with the help of suitable expansions. Among the exceptions is the R -factor R_2 , defined later: the calculation of R -factor derivatives is straightforward in this case.

In fact, a single optimization scheme may not be sufficient: structural searches near the refined solution may need a different method than the initial, coarser and rougher search. Indeed, in any search the parameter space is really explored on two different “length” scales. Firstly, one needs a coarse survey of the large-scale topology of the R -factor hypersurface which allows the search method to locate entrances into R -factor minima and distinguish between distinct local minima. Next, one needs to determine the exact location of a given minimum, for which other methods are more appropriate.

The following methods have been proposed in conjunction with automated optimization schemes to efficiently obtain LEED intensities or derivatives for related structures, and will be described in turn in the following sections:

- tensor LEED within directed-search schemes: this approach is most appropriate for structural refinement;
- a combination of the gradient method (not too close to the minimum) and the expansion method (for refinement close to the minimum);
- linear LEED: this approximate method is most appropriate for a coarse search to explore the existence and approximate location of different minima.

3.1. Tensor-LEED theory

3.1.1. Concepts

The tensor-LEED technique (TLEED) [29–32,21] provides an efficient method for exploring the local regions of the R -factor hypersurface. In its simplest form, called linear tensor LEED (LTLEED), the theory provides the partial derivatives of the diffracted amplitudes with respect to changes in the atomic coordinates; these partial derivatives are gathered in tensors. In its more effective form, called simply tensor LEED (TLEED), one in essence also obtains partial derivatives, but now *with respect to the changes in scattering potential* induced by changes in atomic coordinates.

The theory of TLEED, its validity and applications have been the subject of a recent review article [21]. TLEED is a semi-perturbative approach to the calculation of LEED intensities that starts from a reference structure which is a particular surface structure guessed to be as close as possible to the actual surface structure. This surface is distorted by moving some of the atoms to new positions to generate a trial surface structure which is related to the reference structure by a set of atomic displacements. Examples of a pair of reference and trial surfaces might be an unrelaxed adsorbate structure and a relaxed version of the same structure, or an unreconstructed surface and a particular displacive reconstruction, respectively.

The LEED I - V spectra from the distorted reference structure are calculated by expanding the difference between the diffracted amplitude from the trial and reference surfaces in terms of the atomic displacements. This leads to a very efficient method for the repeated evaluation of the LEED I - V spectra for many trial structures, since many complex trial surface structures can be related to a single reference structure. This approximation gives accurate structural solutions for atomic displacements within a few tenths of an ångström from the reference structure. Thus, TLEED allows the rapid exploration of complex surface relaxations and reconstructions.

Insight into the principles behind TLEED theory can be obtained in the kinematic limit, in which the amplitude of diffraction from beam \mathbf{k} to beam \mathbf{k}' is:

$$A_0(\mathbf{k}, \mathbf{k}') = \sum_{j=1}^N f_j e^{i(\mathbf{k}-\mathbf{k}') \cdot \mathbf{r}_j}. \quad (1)$$

If some of the atoms are moved from their positions \mathbf{r}_j in the reference structure to the positions $\mathbf{r}_j + \delta\mathbf{r}_j$ in some trial structure, then the change in the amplitude of diffraction is, approximately:

$$\delta A(\mathbf{k}, \mathbf{k}') \approx - \sum_{j=1}^N i f_j (\mathbf{k} - \mathbf{k}') \cdot \delta\mathbf{r}_j, \quad |\mathbf{k} - \mathbf{k}'| \cdot \delta\mathbf{r}_j \ll 1. \quad (2)$$

3.1.2. Linear tensor LEED

In the kinematic case, the change in amplitude is *linear* for small atomic displacements $\delta\mathbf{r}_j$. This encourages one to seek a similar linear expansion in the fully dynamical case. This can be done [32] and is the linear tensor-LEED (LTLEED) approximation for the change in the amplitude of a diffracted LEED beam:

$$\delta A \approx \sum_{j=1}^N \sum_{i=1}^3 \mathcal{F}_{ij} \delta r_{ij}. \quad (3)$$

Here, the index j is summed over all N displaced atoms in the reference surface and the index i is summed over the three Cartesian coordinates of each atomic displacement ($i = x, y, z$). The quantity \mathcal{F} is a Cartesian tensor that can be evaluated by a single fully dynamical calculation (at each energy) for the reference structure only. Once \mathcal{F} is determined, I - V spectra for many related trial structures can be evaluated by simply resumming eq. (3): a very efficient numerical procedure.

3.1.3. Tensor LEED

Clearly, this linear approximation has a limited radius of convergence [21], typically 0.2 Å. The approximation fails because, even in the kinematic case, it inadequately represents the change in the surface-scattering potential, δV , produced by displacing an atom. This deficiency is corrected by a more sophisticated version of the theory, called simply tensor LEED (TLEED), which allows the exploration of larger displacements of up to about 0.4 Å. In this case, the relationship between the change in amplitude and the atomic displacements appears in a functional, rather than linear, form in an angular momentum basis:

$$\delta A = \frac{1}{N} \sum_j \sum_{\ell m, \ell' m'} \mathcal{F}_{\ell m, \ell' m'}^j \mathcal{S}_{\ell m, \ell' m'}(\delta\mathbf{r}_j). \quad (4)$$

The quantity \mathcal{S} is a function of the atomic displacements alone; the tensor \mathcal{F} depends only on the reference surface structure.

This expression is correct to all orders of $\delta\mathbf{r}$ and shares with LTLEED the fundamental computational advantage of this approach: once \mathcal{F} has been calculated for the reference structure, it is possible to evaluate I - V spectra from any trial structure by evaluating the matrix \mathcal{S} for each displaced atom and resumming eq. (4).

3.1.4. Accuracy of TLEED

The finite radius of convergence of the more sophisticated version of the TLEED approximation is determined by the extent of multiple scattering correlations between displaced atoms in the trial structure. If the atomic displacements are small, then the magnitude of the change in potential produced by an atomic displacement will be much smaller than the full atomic potential and the neglect of such correlated paths is a good approximation. For displacements larger than a few tenths of an ångström these paths begin to make an important contribution to the scattered intensity and the TLEED approximation worsens. Note that TLEED is exact in the kinematic limit, however, i.e. the radius of convergence becomes infinite in the single-scattering case.

A primary reason for the success of the TLEED approximation is that the relative importance of correlated multiple-scattering paths is reduced by the limited mean free path of the LEED electron within the surface. This means that multiple scattering between atoms farther than a few ångströms apart is negligible, whatever the magnitude of δV . A similar argument may be applied to contributions to the scattered intensity from scattering paths on which an electron returns to the same displaced atom more than once. Such closed loops form a very small proportion of the total number of possible scattering paths and on such paths an electron must undergo backscattering from the atoms surrounding the displaced atom, a weak process.

The radius of convergence of the TLEED approximation depends upon two factors, both of which influence the relative importance of the correlated multiple-scattering paths discussed above. The approximation tends to worsen as the electron energy is increased, a reflection of the decreased wavelength and the increased electron mean free path in the surface. This effect is somewhat compensated for by the decrease in intralayer scattering for higher incident energies. In addition, the radius of convergence shrinks for strong scatterers which produce strong multiple scattering (such as high- Z atoms) and expands for weak scatterers (such as low- Z atoms). In practice, the radius of convergence of TLEED has been determined empirically from the numerous applications of the technique for typical electron energy ranges. For materials in the middle of the Periodic Table, such as Ni, Cu, Pd, Mo and Rh, the radius of convergence is typically about 0.4 Å. For heavier materials, like W, it is around 0.3 Å, and for Pt closer to 0.2 Å. For lighter atoms, such as C, N and O, and especially H, the radius of convergence increases well beyond 0.5 Å. These results indicate a general trend to smaller radii of convergence as one descends the Periodic Table: a straightforward reflection of the general increase in the atomic scattering cross-section with atomic number.

3.1.5. Efficiency of TLEED

The relative simplicity of the mathematical operations required to evaluate intensities for many trial surfaces using TLEED theory has important computational implications. Firstly, the calculation is very fast compared to conventional fully dynamical methods. For instance, by using TLEED theory, the computational time per trial structure can be reduced by a factor of 50 for a simple surface such as Cu(100) and by a factor of 10 000 for a $p(2 \times 2)$ overlayer

system. Secondly, the time taken to evaluate intensities by TLEED is independent of the presence or lack of symmetry within any given trial structure. Therefore, one can consider highly asymmetric systems with no loss of efficiency. These structures are largely inaccessible to conventional methods due to the large volume of parameter space to be explored and the inability to exploit time-saving symmetries. This is especially important when using an automated search, since one cannot exclude that the path to be taken through parameter space by the optimization procedure will pass through asymmetrical trial structures, or indeed that the best-fit structure is asymmetrical.

3.1.6. Applications

To date, surface structures which have been solved with TLEED, coupled with search algorithms mentioned in section 4, include:

- Mo(100)-c(2 × 2)-S [33,34];
- Mo(100)-c(2 × 2)-C [33];
- Rh(111)-(2 × 2)-C₂H₃ [35] (fig. 1);
- Pt(111)-(2 × 2)-C₂H₃ [36];
- Pt(111) [37];
- Pt(111)-(2 × 2)-O [37] (fig. 2);
- Re(0001)-(2 × 2)-S [38];
- β-SiC(100)-c(2 × 2) [39] (fig. 3);
- β-SiC(100)-p(2 × 1) [40] (fig. 4).

The number of optimized structural parameters ranged from 3 to 30 in these structural determinations.

3.2. Nonlinear least-squares fit

3.2.1. Concepts

The least-squares optimization method is based on the minimization of the mean square deviation between experimental and theoretical data points. In order to determine the minimum of the *R*-factor the theoretical intensities are expanded in a Taylor series around the trial structure and the deviation from the trial structure is calculated from the condition that

$$dR_2/dp = 0,$$

where R_2 is an *R*-factor defined later, and p is any parameter to be fit.

In the series expansion only the linear term is used and the fact that the intensity is a highly nonlinear function of the parameters is overcome by iterating the process until convergence is reached. The method requires the knowledge of the partial derivatives of the intensities with respect to the variable parameters rather than the derivatives of the *R*-factor function.

3.2.2. Calculating derivatives

The calculation of derivatives can be done either numerically or analytically. A numerical calculation is in any case appropriate, but time consuming. The computing time scales linearly with the number of parameters and this step quickly becomes the most time-consuming part in the whole analysis. More advantageous would be analytic derivatives, which, however, are not available, but different approximations are possible. In the linear tensor-LEED method described above, the tensor contains in essence the derivatives and these could be used in connection with the expansion method. Nevertheless, to apply the method to all structural and non-structural parameters, e.g. inner potential, temperature factors and random alloy

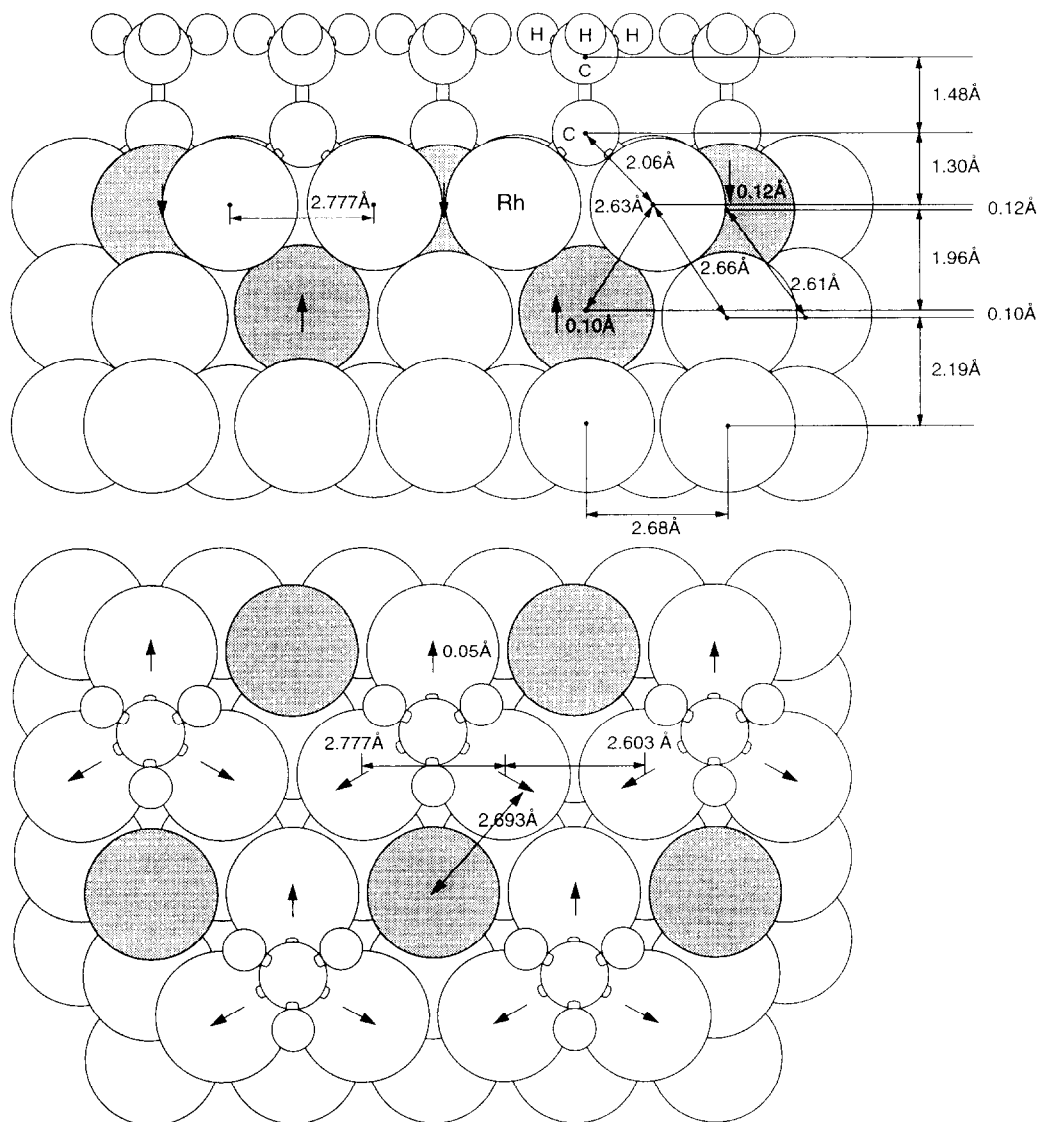


Fig. 1. Side view (top panel) and top view (lower panel) of Rh(111)-(2×2)-C₂H₃ (ethidyne, with guessed H positions). Gray atoms have relaxed perpendicularly to the surface from bulk positions. Substrate relaxations are drawn to scale, emphasized by arrows and labeled by their magnitudes.

concentrations, it is quite useful to have a numerical calculation. Furthermore, using linear expansions and approximations [41], the numerical calculation of derivatives compares favorably with the TLEED method.

The first step for obtaining derivatives is to replace the matrix inversion, which is inherent in the self-consistent solution of the multiple-scattering problem [1,3], by a linear expansion of the matrix elements:

$$\begin{aligned}
 [1 - S(p + \delta p)]^{-1} \\
 = [1 - S(p)]^{-1} + [1 - S(p)]^{-1} [S(p + \delta p) - S(p)] [1 - S(p)]^{-1}.
 \end{aligned}$$

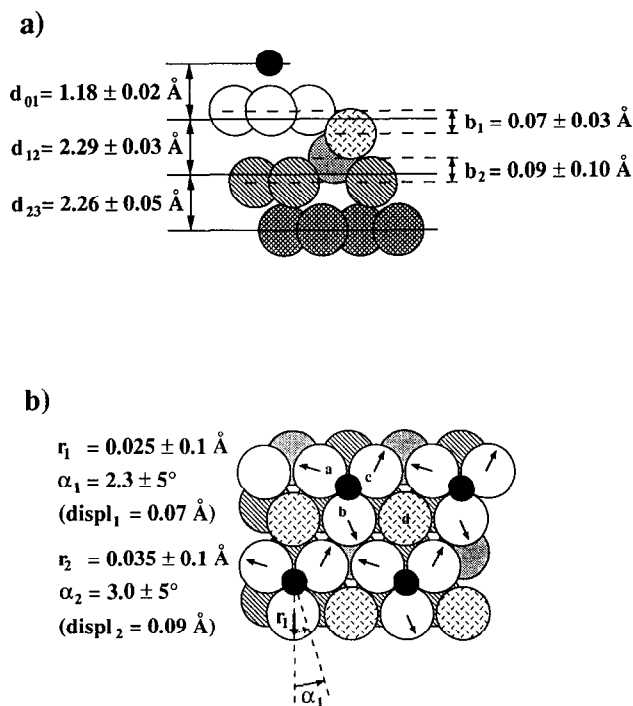


Fig. 2. Schematic side view (a) and top view (b) of Pt(111)-(2×2)-O, including various tested symmetrical distortions. The full bucklings b_1 and b_2 in the two Pt layers can be decomposed in 1:3 proportions to indicate displacements of individual atoms above and below their average planes (shown as full lines in (a)). Vector r_1 represents radial and rotational displacements of the triangles of white Pt atoms which are nearest neighbors to the O adsorbates (shown black) in fcc hollow sites, while vector r_2 represents the corresponding displacements in the second metal layer (cross-hatched Pt atoms); the radial components of these vectors are labeled displ₁ and displ₂.

Here \mathcal{S} is a matrix representing contributions from multiple-scattering paths. This expression can be inserted in the calculation of layer-scattering matrices and in the layer-doubling method [1,3]. The matrix inversion must be performed only once and the related vectors can be stored and re-used again. Only the increment of the lattice sum needs to be recalculated for each positional parameter and one can take advantage of several approximations [41]. The calculation of derivatives does not require the same accuracy as the full calculation of the intensities for the reference structure. The derivatives give the direction in which the atoms must be shifted and the full calculation is repeated for each iteration step. It is therefore sufficient to reduce the number of phase shifts and to reduce the number of lattice points in the lattice sum. A similar reduction is also possible for the set of plane waves in the layer-doubling scheme. The total time required to calculate derivatives then depends only weakly on the number of free parameters.

3.2.3. Applications

This optimization method has been applied to a number of structure analyses:

- Pt₈₀Fe₂₀(110)-(1×2) [42];
- Ni(110)-(2×1)-O [20];
- Co(10 $\bar{1}$ 0) [43];

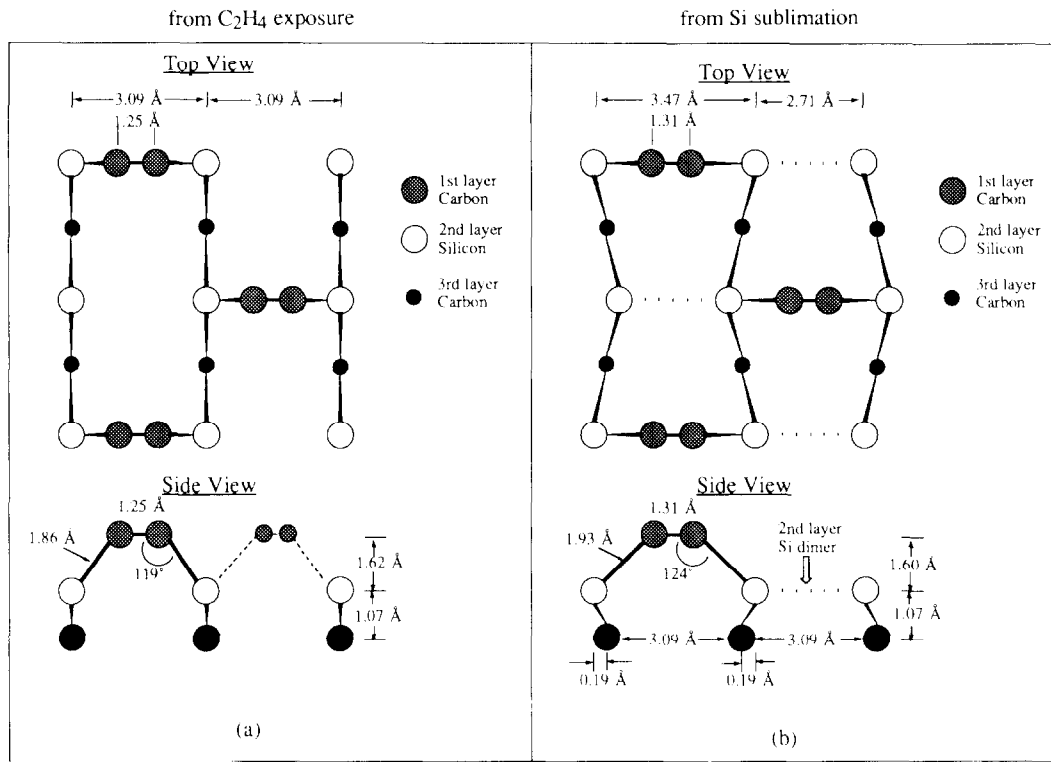


Fig. 3. Two closely related structures for β -SiC(100)- $c(2 \times 2)$, both carbon-rich: (a) as obtained from C_2H_4 deposition, and therefore possibly including hydrogen; (b) as obtained by Si sublimation, and therefore hydrogen-free. Different relaxations are found, especially in the second (Si) layer. Note the formation of symmetrical carbon pairs, qualitatively different from the Si dimers in the Si-rich version of this structure (cf. fig. 4), in that each carbon in a pair has *two* bonding neighbors.

- Ru(0001)- $(\sqrt{3} \times \sqrt{3})R30^\circ$ -Cs and (2×2) -Cs [44];
- Cu(110)- $c(6 \times 2)$ -O [45];
- Ru(0001)- $(\sqrt{3} \times \sqrt{3})R30^\circ$ -O + Cs [46] (fig. 5);
- Ni(110)- (1×2) -H [19];
- Al(111)- $(\sqrt{3} \times \sqrt{3})R30^\circ$ -K [47];
- Cu(110)- (1×2) -H [48];
- Cu(110)- $c(8 \times 2)$ -S [49].

The number of optimized structural parameters ranged from 6 to 26 in these structural determinations.

3.3. Linear LEED

3.3.1. Concepts

Very recently, a new approximate method has been developed, called linear LEED (LLEED), that will be useful to explore larger areas of the structural-parameter space [50]. Its principles are described in more detail elsewhere in this volume [51]. LLEED is aimed particularly at exploring *combinations* of atomic displacements, where several atoms or rigid groups of atoms are displaced simultaneously. These displacements are treated as indepen-

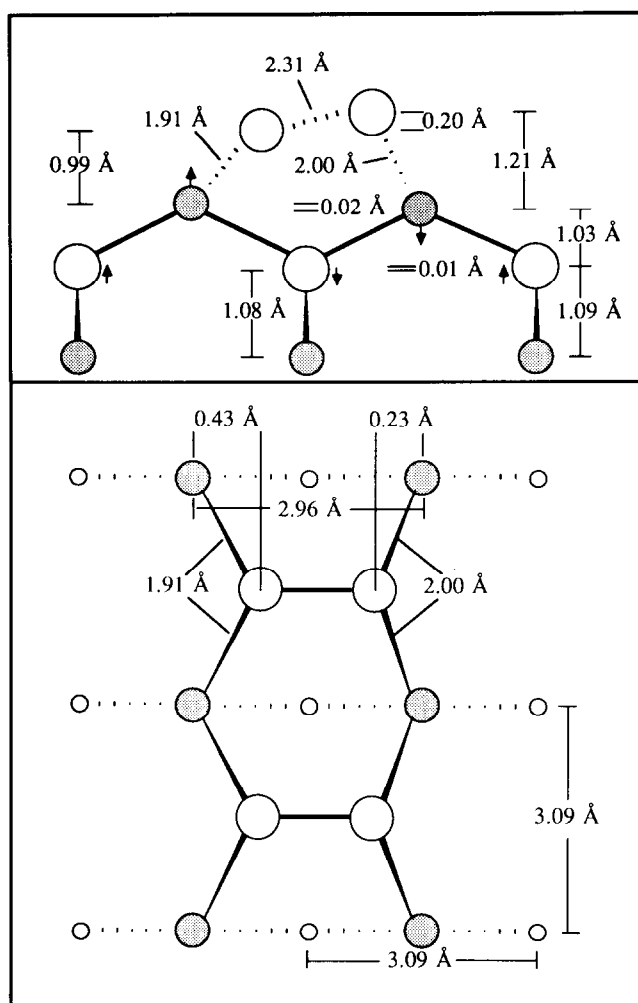


Fig. 4. Side view (top panel) and top view (lower panel) of β -SiC(100)-p(2 \times 1), which is Si-rich as obtained by Si deposition. Note the formation of asymmetrical silicon dimers, similar to those on Si(100)-(2 \times 1) (Si is shown as open circles, C as gray circles); the Si dimers are qualitatively different from the C pairs in the C-rich reconstructions (cf. fig. 3), in that each silicon in a dimer has *three* bonding neighbors.

dent and therefore with great computational advantage. (Note that this advantage disappears for displacements of single atoms alone.)

The label “linear” in linear LEED describes the basic assumption (or approximation) of the method, namely that independent atomic displacements have linearly independent effects on LEED amplitudes (it does not in any way imply a linear expansion for small atomic displacements).

In LLEED a fully dynamical LEED calculation is performed for a particular reference structure, giving an amplitude A_0 for a given diffracted beam. Additionally, a trial structure is considered in which several atoms (or groups of atoms, like molecules), labeled 1, 2, ..., N , have been displaced by arbitrary amounts. As an example with $N = 2$, consider the coadsorption of C and O atoms on Ni(100): assume that in the reference structure the two atoms are in

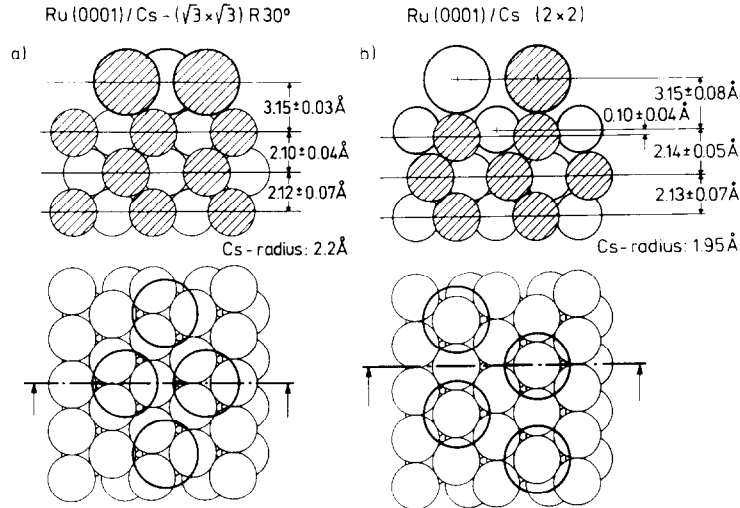


Fig. 5. Side views (top panels) and top views (lower panels) of Cs overlayers on Ru(0001) at coverages of (a) $\theta = 1/3$ and (b) $\theta = 1/4$. Note the change in adsorption site from hollow to top with increasing coverage, and the inward buckling of the metal under the top site.

hollow sites, while in the trial structure both atoms are in top sites. The objective is to obtain the new beam amplitude $A_{12\dots N}$ for that trial structure. To that end, one makes exact fully dynamical LEED calculations of the diffraction amplitudes for a set of N related structures: in each such related structure only one of those atoms (or groups of atoms) is displaced to its trial position. In the current example, one would displace the C atom alone to the top site (leaving the O atom in the hollow site), yielding beam amplitude A_1 , and separately move O to the top site (leaving C in the hollow site), yielding beam amplitude A_2 . In general, N such calculations are needed, yielding N amplitudes A_j , $j = 1, 2, \dots, N$ for the beam in question.

Now the LLEED amplitude for the trial structure with all displacements is, by definition, the following simple linear combination, which is an approximation to the correct amplitude:

$$A_{12\dots N} = A_0 + \sum_{j=1}^N (A_j - A_0). \quad (5)$$

(This equation holds for the beam of interest, other beams being treated in exactly the same way.) In our example, the equation would read

$$A_{12} = A_0 + (A_1 - A_0) + (A_2 - A_0). \quad (6)$$

Thus far, the computation has been made $N + 1$ times more demanding than apparently necessary: one could have computed $A_{12\dots N}$ in one single calculation. However, the advantage of the LLEED method emerges when one allows sequences of atomic or group displacements and then combinations thereof. One generates exact multiple-scattering amplitudes $A_j^{k_j}$ for sequences of single-atom or single-group displacements labeled $k_j = 1, 2, \dots, M_j$ (such as a sequence of C positions and a sequence of O positions in our example). One can then use LLEED to scan very many *combinations* of atomic displacements, by the repeated use of eq. (5), which takes negligible computing time. Thus, all pairwise combinations of C and O positions obtained from their two individual position sequences can be rapidly generated.

Now the big savings in computing time have emerged, and they grow rapidly with the number of parameters to be fit. For instance, consider the case of a simple clean surface in which the top 5 interlayer spacings are varied, with each spacing taking on 10 trial values. Conventional LEED requires fully dynamical calculations for 10^5 different structures. By contrast, LLEED would first calculate and tabulate diffracted-beam amplitudes when only the first of the five spacings is changed, and then when only the second spacing is changed, etc., requiring only $5 \times 10 = 50$ fully dynamical calculations. The 10^5 different relaxed structures are then generated by simple linear combinations of these 50 tabulated terms. The gain in efficiency is more than three orders of magnitude in this instance.

The magnitude of the displacements from the reference structure to the trial structures is largely unlimited (except for the requirement that two displaced atoms should not move so close together that multiple scattering between them becomes extremely strong). In fact, moving atoms far away from each other is advantageous. As a result, LLEED is ideally suited for examining *large* displacements and thus large sections of parameter space. As a consequence, one can efficiently explore on a coarse parameter grid the presence and approximate locations of different *R*-factor minima. The exact minima locations can then be determined with other refinement techniques that are more effective on the fine scale.

Note that (in contrast to TLEED, for instance) LLEED cannot treat different coordinates of the same atom as independent parameters: LLEED requires one fully dynamical calculation for each three-dimensional position of an atom (or group).

3.3.2. Accuracy of LLEED

The LLEED approximation involves only the neglect of corrections to certain multiple-scattering paths: those with two or more scatterings from different displaced atoms (TLEED neglects corrections to these and further multiple-scattering paths, and is therefore slightly less accurate for comparable structures). The fact that these paths contribute relatively little ensures that LLEED performs with remarkable accuracy. Note that LLEED becomes exact in the kinematic limit. Tests have shown the approximation to be remarkably good even for surfaces composed of such strongly scattering atoms as Pt. The LLEED approximation improves when the independently moving atoms are distant from each other (since no multiple-scattering paths connect them). As a function of atomic displacements, the LLEED error increases to a relatively small value after perhaps 0.5 \AA , which error remains approximately constant thereafter.

3.3.3. Potential applications

LLEED promises to be particularly useful in at least the following three separate areas of research. Firstly, as explained above, the method serves as an ideal complement to those perturbative schemes, like TLEED, which perform best at small atomic displacements: LLEED works best for a coarse and wide-ranging exploration of parameter space. The LLEED scheme has, however, so far not been applied in any structural determination, so its exact practical potential remains to be studied.

Secondly, the LLEED method offers the prospect of studying new classes of complex structures previously beyond the reach of LEED. These include systems with compositional and lateral disorder. For example, consider an epitaxial system in which the overlayer grows as islands small relative to the coherence length (i.e. instrumental response function) of the LEED beam, and such that the internal structure of the islands is incommensurate with the substrate lattice. Unlike conventional LEED, the LLEED method can be used to investigate such systems. The LEED electronic state generated by the islands can be constructed as a

linear combination of amplitudes resulting from overlayer atoms being placed further and further away from their equilibrium position, with unknown coefficients to be fit to the data. This should enable the extraction of information about properties such as the maximum island size [52].

Thirdly, a more tentative possibility exists. Methods such as direct inversion of electron holography rely on the linearity of the underlying mathematical schemes. The introduction of a linear approximation into conventional dynamical LEED may open up new and exciting prospects of directly inverting conventional LEED data [51].

4. Search algorithms

4.1. Types of search methods

The objective of structural optimization is to find the minimum of a LEED R -factor as a function of the structural parameters, and as a function of non-structural parameters (such as the muffin-tin zero). Many optimization algorithms have been introduced over the years: they differ in their requirements (e.g. possible need for partial derivatives of R -factors or intensities) and performance (e.g. efficiency on complicated hypersurfaces and near minima). Since R -factor partial derivatives cannot be obtained analytically in LEED, only optimization methods can be applied which tolerate numerically computed derivatives or do not require derivatives. Derivatives are also sensitive to effects like experimental noise and computational truncations, thereby endangering any search based on derivatives.

Regarding performance, it is likely that a combination of optimization methods will be best, as in the Marquardt approach (see section 3.2): one method first explores wider areas of parameter space, then another refines parameters closer to the preferred minimum. Methods to explore different minima in order to select out the global minimum are available (such as simulated annealing [53], which makes large random jumps in parameter space), but are likely to be efficient only in combination with very rapid LEED approaches, at this point in time perhaps only LLEED. However, the issue of finding the global minimum will always remain difficult (as it is in X-ray crystallography with structures of a complexity such that its direct methods cannot be applied).

For LEED analyses, the following optimization schemes have been implemented, which we shall discuss in this section:

- direct methods [54];
- the least-squares approach [55,53];
- the simplex method [53];
- the Hooke–Jeeves algorithm [15,16], a form of steepest descent [53];
- the Rosenbrook algorithm [56], and a modification of the Rosenbrook algorithm [53];
- the direction-set method [53,57].

4.2. Direct methods in LEED

Compared to LEED, an advantage of X-ray crystallography is its ability to exploit *direct methods* which originate from the simple analytic relationship between the diffracted amplitude and the crystal structure [58]. However, until recently, LEED had resisted the application of direct methods, due to strong elastic multiple scattering and the complex nature of electron–atom scattering. In particular, LEED spectra are not amenable to Fourier synthesis

because, in X-ray terms, the effective form factors of the surface atoms are complex and have a different phase for each inequivalent atom in the surface. Thus the Fourier-transform methods interpret phase differences introduced by atomic and elastic multiple scattering as changes in atomic coordinates. This gives rise to spurious features in real-space transforms [59].

Recently, however, Pendry and co-workers have proposed a direct method for LEED, based upon tensor-LEED theory [60–63,54]. The fundamental idea is not to attempt a complete inversion of a set of $I-V$ spectra, but instead to consider the difference between the measured $I-V$ spectra and those calculated for a guessed reference surface. The direct method then takes the difference between the measured $I-V$ spectra and those calculated for the reference structure and uses it to directly determine how the actual surface structure deviates from that of the reference surface.

Pendry and co-workers have applied this approach to the determination of the interlayer spacings and adsorption heights for several simple systems: Rh(110), Rh(110)-(1 × 1)-2H, W(100) [60], Ni(100)-c(2 × 2)-O [54,63], Ni(100)-p(2 × 2)-O [63] and Ni(100)-c(2 × 2)-S [63]. In each of these cases the reference structure was the bulk termination of the solid and the displacements directly determined were 0.1 Å or less. This was necessary because this version of the direct method employs the linear version of tensor-LEED theory which fails for larger displacements. A more sophisticated scheme, based on the full tensor-LEED theory, has been proposed and applied to one test case [64]. In principle, this development should enable the application of the direct method to surfaces in which the actual atomic positions deviate by more than 0.2 Å from their positions in the reference structure.

Despite this development, the direct methodology has a number of disadvantages compared to more conventional methods. Firstly, it requires the comparison of absolute experimental and theoretical intensities, a generally undesirable procedure since it is well known that static and dynamic disorder within the surface usually leads to significant disagreement between the absolute intensity of calculated and experimental $I-V$ spectra. While this deficiency can be overcome by using R -factor methods, this would add significantly to the complexity of the method and the inversion procedure. In addition, the direct method requires the solution of an overdetermined set of simultaneous equations which relate the intensity differences to the atomic displacements (typically there are many times more experimental energy points than structural parameters to be determined). This represents a difficult and unstable numerical problem which has no exact solution. Its solution requires sophisticated and time-consuming computational techniques.

A potential advantage of these direct methods is that, in principle, they avoid the problem of local versus global minima. Thus, although the initial results of this approach appear promising [65], the direct method requires further development before it can be considered as a reliable alternative to trial-and-error or optimization methods.

4.3. Marquardt approach

A very efficient optimization scheme is the so-called expansion method which is routinely applied in many fields and is also the standard method used in X-ray structure refinement. It is based on the minimization of a fitting function which is usually the mean square deviation between experimental and theoretical data points. It requires the knowledge of the derivatives of the intensities with respect to the variable parameters. In its original form it works well near the optimum where the gradient is small, because it is based on a linear expansion of the

intensities as a function of the variable parameters. Far away from the optimum, the gradient methods usually work better.

Therefore, a combination of both methods has been developed by Marquardt [55] and his approach has in fact become the standard method for optimization. With LEED it has been successfully applied in a number of structure analyses [19,20,42–48]. Detailed descriptions of the procedure can be found in most textbooks [53]; we outline the method below.

The quantity which is minimized is the mean square deviation between the normalized intensities, summed over energies:

$$R_2 = \sum_i (I_e^i - I_t^i)^2.$$

A linear expansion of the intensity function in terms of a change in a parameter p to be fit,

$$I(p_m + \Delta p_m) = I(p_m) + \frac{\partial I}{\partial p_m} \Delta p_m,$$

can be inserted into the minimum condition,

$$dR_2/dp_m = 0,$$

leading to a set of linear equations which defines the change Δp :

$$\sum_i \left(I_e^i - I_t^i - \sum_j \frac{\partial I_t^i}{\partial p_j} \Delta p_j \right) \frac{\partial I_t^i}{\partial p_m} = 0,$$

or, in short form:

$$\beta_m = \sum_j \Delta p_j \alpha_{jm}.$$

Replacing the coefficients α_{jm} by $\alpha_{jm}^0 = \alpha_{jm}(1 + \delta_{jm}\lambda)$, allows a continuous transition from a gradient-method-like behavior (large values of λ) to the expansion method (small values of λ). The parameter λ is dynamically adjusted.

It should also be noted that the method is not limited to minimizing the mean square deviation as described above. One may also use the Y -function as defined by Pendry [66] (see section 5.4). In that case it is necessary to use a step width on the energy scale which is sufficiently small to calculate the Y -function, since the Y -function requires the derivatives of the intensities with respect to energy. The Y -function is defined for single energy points and the derivatives dY/dp can be calculated numerically using a small increment in the parameters. Using the Y -function as criterion, the method is closely related to the direct method in combination with the linear tensor-LEED method [29]. The results should be close and a detailed study comparing both methods is in progress.

4.4. Simplex method

Among the simplest optimization algorithms is the simplex method [53,37]. It does not require derivatives at all, but uses a “simplex” (set of vertices) of $N + 1$ points in parameter space, if there are N parameters to fit. At each iteration step, the vertex with the highest R -factor is replaced by a new vertex guessed to provide a lower R -factor. It is a very robust, if not rapid method: in test cases, it seems to be considerably slowed down by the presence of long, shallow, twisting valleys in the R -factor hypersurface.

4.5. Direction-set method

A more effective algorithm is the direction-set method [53,57,37], which minimizes the R -factor along a set of independent directions which are updated as the search proceeds. The minimization along each direction is done independently, by parabolic interpolation if the function is tested to be parabolic in the region of interest, or by simple bracketing if such a test fails. In order to optimize the efficiency of this step the algorithm updates the directions by trying to converge on a set of so-called conjugate directions, which are such that minimization along one does not spoil the subsequent minimization along another. As an example, if we consider minimizing a positive, quadratic function, a possible set of conjugate directions (but not the only one) corresponds to the eigenvectors of the matrix A defining the quadratic function. If these, say N , eigenvectors are identified, the problem is reduced to N one-dimensional independent minimizations along each direction.

4.6. Rosenbrook method

The Rosenbrook algorithm [56,33], as well as its modification [53], is best used when the search has already reached the vicinity of a local minimum. It identifies a set of conjugate directions by periodically computing the Hessian matrix of the R -factor (the Hessian is the matrix of partial second derivatives) and by updating the set of conjugate directions to the set of principal directions of the Hessian. This option returns the position of the minimum together with the principal directions and the corresponding curvatures of the R -factor at the minimum: these are useful information for evaluating the uncertainties of the structural determination.

4.7. Hooke–Jeeves method

The Hooke–Jeeves approach [15,16] is a form of steepest-descent method [53]. It explores the local shape of the R -factor hypersurface in the immediate vicinity of a given structure, and deduces from it the best direction in which to move in order to reduce the R -factor value. The search proceeds in that direction until the R -factor no longer diminishes. The scheme is then repeated from the new point reached in this manner. This scheme was employed in a LEED structural determination which used full-dynamical calculations for all R -factor evaluations needed in the process [16]. It could be considerably accelerated by applying TLEED or other methods.

5. Practical issues

In this section, we address the practical use of the methods described above, with emphasis on experience gained with them in determining actual surface structures with LEED. These issues are important in view of the increasing automation of structural determination and in view of the resulting reliability that one may expect.

A first issue is the level of automation that one can hope to achieve. Complete automation is not possible, as shown with the case of X-ray crystallography. We expand on this in section 5.1.

Solving structures in much more detail than before (e.g. fitting 30 structural parameters) raises the question of the achievable accuracy. Clearly, fitting many parameters allows a closer

fit between theory and experiment, but this is only meaningful if the theoretical ingredients are accurate enough, as discussed below in section 5.2, and if the experimental database is adequate, as discussed in section 5.3.

There is also the question of which R -factors are appropriate for the task, an issue we address in section 5.4. The practical performance of optimization methods is reviewed in section 5.5. And finally, in section 5.6, we discuss the difficult problem of assigning an uncertainty to the best-fit parameters.

5.1. Achievable level of automation

It is important to realize that a structure determination never can be a fully automated process. Instead, a human being must first be closely involved in the generation and selection of model structures to try out. Such models will be based on accumulated knowledge about the structure, as obtained by all sorts of methods. For instance, knowledge of the chemical composition of the surface is essential (from Auger electron spectroscopy or thermal desorption spectroscopy). Topography may be available from scanning tunneling microscopy. Molecular-species identification and approximate molecular orientation may be given by vibrational measurements. Bond lengths and angles have to satisfy well known criteria. Previous structural determinations and theory, for the same or similar systems, may provide models or model ingredients for investigation.

Then, the fitting of parameters is often done in separate stages: one would first fit parameters on which the diffraction intensities depend strongly (like coordinates perpendicular to the surface), and one would only then add other less sensitive parameters in one or more new fitting processes. One may also start with optimizations that maintain a high structural symmetry, before exploring lower-symmetry structures in separate optimizations.

Often, searches based on the initial list of models do not yield any acceptable structure. Then one must go back to propose other models, question any assumptions, or perhaps check the surface preparation and the experimental methods.

When an acceptable structure is obtained, it is still advisable to iterate the optimization process at least once in order to make sure that any approximations used in the LEED calculations (as in TLEED and expansion methods) have not shifted the R -factor minimum away from the actual correct location. It is also necessary to verify that the search has actually reached a minimum (rather than a saddle point allowing further minimization). This involves running a sequence of similar parameter optimizations starting from different trial structures in the neighborhood of the presumed correct structure.

Also, it is advisable to perform further optimizations with different atomic scattering potentials and other non-structural parameters (if not fit previously).

Full automation applies thus only to the process of optimizing once a set of structural and/or non-structural parameters. Many such optimization processes are involved in a typical structural determination, and they must be selected by a human being as the analysis proceeds. Human intervention also provides a frequent and beneficial check on the progress of the search.

5.2. Required quality of LEED theory

5.2.1. Quick and rough searches

It can be profitable to perform a quick and rough structural determination on the basis of a less-than-accurate theory, especially in the early stages of a coarse search for approximate

structures to be refined later. (This could be usefully combined with the LLEED scheme.) Such an approach can drastically cut the computing time, e.g. when a smaller angular-momentum cut-off l_{\max} or fewer plane waves are used than otherwise needed. For instance, with Pt(111), cutting l_{\max} from 9 to 6 for the energy interval 50–250 eV affects the best-fit topmost interlayer spacing by less than 0.02 Å, although intensities change appreciably. However, one must then be cautious not to reject structures giving apparently incorrect local minima: the intentional theoretical inaccuracies can easily make the correct global minimum look like a local minimum.

5.2.2. Lattice parameters

Rarely discussed, and never explored to our knowledge, is the uncertainty in the lattice parameters used in LEED analyses to set the unit-cell parameters in the surface plane: one normally takes bulk-lattice constants from structural tables, but such tabulated values can vary by 1% or more (representing a variation by 0.02–0.03 Å for the interatomic distance between close-packed atoms). The resulting uncertainty on atomic locations could be comparable to this lattice-constant uncertainty. This obviously could have serious implications on refined structure determinations approaching 0.01 Å in accuracy.

This issue may become even more dramatic in situations where epitaxially grown films are investigated. A lattice misfit leads to stress and gradual change of the lattice parameter with film thickness. In such cases the lattice parameters may have to be included among the search parameters.

5.2.3. Atomic scattering amplitude

Recent work is pointing to the need to pay closer attention than heretofore to the atomic scattering amplitude (phase shifts) used in LEED, when trying to optimize many structural parameters with high accuracy [37]. It is, however, not yet possible to systematically quantify the effects of theoretical uncertainties on the best-fit atomic coordinates. We shall in this section review some findings in this domain.

A number of investigations fortunately point to a lesser sensitivity of best-fit structural parameters to the atomic scattering than do the LEED intensities themselves. For instance, substituting Co for Ni phase shifts (Co and Ni are adjacent in the Periodic Table) would have a negligible effect on the best-fit structure [67]. However, the method of preparing the atomic scattering potential could introduce larger uncertainties. For example, using a free-atom potential as opposed to a solid-state atom could introduce structural errors in excess of 0.02 Å. Experience with Pt indicates that structural parameters can vary by 0.01–0.03 Å, as one varies the method of calculating the exchange contribution.

Relativistic effects have always been known to play a role in LEED for heavy elements, e.g. in the 5d row of the Periodic Table, especially as far as LEED intensities are concerned. Such effects should enter at least at two stages in the calculation: in the computation of the atomic charge densities needed to obtain the muffin-tin potential, and in the calculation of the phase shifts from the muffin-tin potential. It is now routine to include relativistic effects by solving the Dirac equation for the free atom (or ion) rather than the Schrödinger equation within the Hartree–Fock approximation. (The codes available today for the free-atom problem do not even require a local-exchange approximation, but treating atomic exchange exactly does not make any appreciable difference, if one is simply interested, as we are, in the total charge density.) Phase shifts can be obtained by solving again the Dirac equation in the presence of the spherical muffin-tin potential (a spin average is needed in this case to produce the phase

shifts used in LEED programs, which, for the most part, do not include spin dependence in the LEED wavefunctions).

We find that relativistic effects may not change the optimal structure of a heavy element itself, but that they can markedly change the positions of light atoms in the same structure. For instance, for clean Pt(111), one finds that the inclusion of relativistic effects does not change the optimum structure by more than about 0.01 Å, while it can considerably improve the $I-V$ curve fit. It turns out that the most important step is the relativistic phase-shift calculation, as can be inferred by the values 0.3, 0.32, and 0.19 for R_p (the Pendry R -factor) as we progressively include the effects previously mentioned. By contrast, the effect on the structure of Pt(111)-(2 × 2)-O is much larger: the best-fit Pt–O spacing decreases from 1.26 to 1.19 Å, a change of 0.07 Å.

At present, practically all LEED calculations are performed within the muffin-tin approximation. It makes the assumption that the atomic ion cores do most of the scattering and that the interstitial potential is sufficiently slowly varying that it may be averaged to a constant (the muffin-tin zero). This approximation becomes less accurate as the electron energy decreases, but is nevertheless successful even near and below the Fermi level, where it forms the basis of the KKR [68,69] and SW- $X\alpha$ methods [70] for the evaluation of the electronic structure of solids and molecules. Where the muffin-tin approximation is least accurate is in the treatment of the molecular scattering, because in molecules a substantial fraction of the total electronic charge density resides between the ion cores. Accuracy of molecular coordinates will therefore lag behind that of more close-packed materials; one should expect a several-fold reduction in accuracy, unless more complex non-spherical scattering potentials are introduced.

5.2.4. Relative importance of non-structural parameters

For the other non-structural parameters, an older, detailed study of Pt(111) [71] gives a useful idea of their relative importance. The relative error bars quoted for the one structural parameter and three non-structural parameters were: 0.44% for the topmost interlayer spacing, 10.5% for the muffin-tin zero, 8.1% for the imaginary part of the inner potential and 5.3% for the Debye temperature. Thus, the sensitivity to non-structural parameters can be as much as 10 times lower than that to structural parameters. This, on the other hand, of course means that their influence on the structural search result is relatively small.

5.2.5. Muffin-tin zero

The muffin-tin zero (often loosely termed inner potential) is always used as a fit-parameter and is included in the optimization procedure as a simple relative shift of the experimental and theoretical $I-V$ spectra (for this reason it is advisable to compute the theoretical $I-V$ spectra over a wider range of energies than provided by the experiment, in order not to lose data at the end points). Usually an energy-independent muffin-tin zero is assumed, resulting in a rigid shift. It is important not to constrain the muffin-tin zero to a coarse grid of values, but to allow continuous changes; otherwise multiple closely spaced minima may result.

An optimization of the weak but accepted energy dependence of the muffin-tin zero has not been tried with an automatic fit procedure. With the conventional trial-and-error approach, this fitting usually leads to an improvement of the R -factor, but has little influence on the structural parameters.

5.2.6. Damping

Structure determination by LEED is quite *insensitive* to uncertainties in the imaginary part V_{oi} of the inner potential (i.e. the damping, also described by the mean free path). As an

example, varying V_{oi} from -1 to -10 eV (its optimum value being about -5 eV) affects the Pendry R -factor, but not the structure of Pt(111) on the scale of 0.01 Å.

5.2.7. Thermal vibrations

Thermal vibrations have been optimized in LEED within the familiar Debye approximation. One finds considerable structural *insensitivity* to uncertainties in thermal effects, especially at low temperatures. For instance, with Pt(111), a change of as much as 60 K in the Debye temperature has no effect on structure on the scale of 0.02 Å. (However, one cannot draw conclusions about thermal vibrations from such results, because the treatment of thermal vibrations in the multiple-scattering theory is inadequate. For instance, correlations in the vibrations between atoms are neglected, although they are known to be strong [1].)

By comparison, in X-ray structure analysis the structure refinement usually starts with an overall isotropic temperature factor and determines the positional parameters. If reflections with high momentum transfer are measured, these may be omitted at this stage, because wrong temperature factors have a strong influence on the high-index reflections. After determining the positional parameters, *isotropic* thermal vibrations are refined and only then *anisotropic* vibrations for each atom. At this stage the high-index reflections must be included. The intensity R -factors may drop from 0.1 – 0.2 for an overall isotropic temperature factor to about 0.02 – 0.05 for individual anisotropic temperature factors. The initially determined positional parameters change very little in the final refinement. However, if the high-index reflections were included in the initial stage, the influence on the positional parameters would be larger and may reach, say, 0.05 Å. It must also be mentioned that the determination of thermal vibrations with X-rays has its limitations: the high-index reflections which are required for this analysis frequently have systematic errors due to absorption effects and need to be corrected.

A comparison with LEED, where because of the backscattering geometry a high momentum transfer normal to the surface normally exists, leads to the conclusion that the precision of the analysis done with isotropic thermal vibrations is an underestimate. In the case of X-rays the R -factor drops significantly after introducing anisotropic thermal vibrations. We can expect the same for LEED. How much this influences the interatomic distances, layer spacings, etc., needs to be investigated and cannot be seriously evaluated today.

5.2.8. Optimizing non-structural parameters

Given the influence of certain non-structural parameters in the LEED determination, one possible way forward is to attempt to include these quantities in the optimized search. In doing this we are faced with the same problem encountered when searching for structural parameters: we require an efficient method of evaluating I - V spectra as the non-structural parameters are varied. In many cases, TLEED theory provides a means of doing this since a change in the non-structural parameter can be interpreted as a change in the scattering potential of the surface amenable to the type of perturbation approach exemplified by TLEED. A good example is that of anisotropic vibrations of surface species which can be directly treated with linear TLEED [72]. In principle, it is also possible to use TLEED to treat variations in the atomic scattering potential. In this way, the atomic scattering amplitude could be refined within an optimized search. A nice feature of the TLEED approximation is that there is no requirement for the potential variation to be spherically symmetric. Thus TLEED may allow us to go beyond the muffin-tin approximation towards a full-potential LEED theory. TLEED can also be extended to other perturbations, such as weak-atom scattering and spin-dependent scattering.

Derivatives of the intensities with respect to non-structural parameters can also be calculated numerically or using combinations of numerical and analytical methods, depending on the type of the parameter [41]. Thermal vibrations within the Debye model, variation of the scattering potential and a variation of the concentration within the average t -matrix approximation (ATA) are relatively simple to calculate because the main effort lies in the calculation of the interatomic electron propagators which are unaffected by a variation of the atomic t -matrices.

5.3. Required experimental database

The most critical experimental conditions affecting LEED-intensity measurements and having consequences on structure determination include:

- the angle of incidence (and its dependence on magnetic fields); this may be one of the most important causes of systematic experimental errors in LEED, particularly for off-normal incidence;
- cleanliness and purity of adlayers (when impurities affect the structure);
- coexistence of other phases, especially such phases containing the same periodicities as the phase of interest;
- preferential domain orientations that lower the symmetry of the LEED pattern.

Less critical conditions are:

- the surface temperature (as long as no phase transitions are inadvertently introduced);
- defects such as ordered or disordered steps and impurities that do not affect the structure.

We next discuss several aspects of experimental data that affect structure determination.

5.3.1. I - V -curve smoothing

Smoothing experimental I - V curves to reduce random noise is usually necessary, especially when R -factors are used that require the first or second energy derivatives of the intensities. Generally speaking, however, the primary effect of smoothing is to markedly lower the R -factor, with relatively little impact on the best-fit structure. One or two successive smoothings generally suffice. Some methods of smoothing not only remove noise, but also modify the underlying curve shape: one may therefore, for consistency in such cases, smooth the theoretical I - V curve in the same manner (this should be done on the same energy grid).

5.3.2. Database size

As mentioned before, the number of significant data points in I - V curves is often taken to equal the number of maxima. Using data at normal incidence over a typical energy range (e.g. 50–200 eV), one usually gets an overdetermination of parameters by a factor 5–10, which is comparable to the case of X-ray crystallography. Thus, such an overdetermination factor can be safely adopted in automated structure analysis by LEED.

It should be noted that the number of free parameters is given by the structure and the penetration depth, i.e. by the number of independent atoms sensed by the LEED experiment. Determining only a few parameters, e.g. only one or two interlayer spacings, does not imply that fewer data points should be used, since that would reduce the precision in addition to the loss of accuracy due to artificially fixing certain parameters.

5.3.3. Off-normal incidence

If more data are desired than are available at normal incidence, one can turn to off-normal incidence and record many times more data points. One present problem with this is that off-normal incidence angles are difficult to measure accurately enough with current equipment: goniometers would be needed, or else the incidence direction should be made adjustable in the search procedure. (Normal incidence is relatively easily set when the LEED pattern exhibits sufficient symmetry; but this is not the case for low-symmetry structures like stepped surfaces, for instance, where no symmetrically equivalent domains exist to symmetrize the observed pattern.) Another disadvantage of off-normal incidence relates to domains: LEED calculations must then be performed separately for each equivalent domain orientation and then averaged together, since the incidence directions on different domains will no longer be equivalent. This complicates an automated search procedure considerably.

It should be noted that measuring at two slightly different angles of incidence gives data that are not fully independent. In practice, one can expect strong dependence between I - V curves taken at angles that differ by an amount that can be generally characterized as follows: less than a tenth of the angles between adjacent integer-order beams on common close-packed metal surfaces [73].

5.3.4. Use of subsets of data

There are cases where a subset of data can be used profitably in a structural determination. One instance is to independently optimize the structure with different subsets of beams or different energy ranges and to contrast the results: the discrepancy between results provides an estimate of structural error bars and of the reliability of the structural determination.

Another example is the analysis of hydrogen superstructures which only weakly influence the integer-order beams but strongly the fractional-order beams. The analysis of the fractional-order beams then enhances the significance for the correct structure model.

Similar findings apply to superstructure-inducing displacive relaxations, such as layer bucklings and periodicity-breaking lateral relaxations. The integer-order beams are often relatively insensitive to relaxations induced by adatoms, while fractional-order beams are strongly affected. In fact, optimizing the structure on the basis of integer-order beams only may yield a poor fit for the fractional-order beams, whereas an all-beam optimization can give good fits in all beams [37].

5.4. R -factors

In contrast to the case with X-ray crystallography, many different R -factor definitions have been used in LEED [3,74], there being no consensus on which is most appropriate. In combination with search algorithms, the primary R -factors used so far have been R_p (the Pendry R -factor), and R_2 (the most common X-ray R -factor). The otherwise popular Zanazzi–Jona R -factor, R_{ZJ} , suffers from higher computational costs and has been found to behave somewhat less predictably than other R -factors in conventional structural determination: it may therefore be less safe to use in an automated search algorithm.

5.4.1. R -factor definitions

We here briefly define the R -factors referred to in this article; more complete explanations can be found in the literature [3,74]. One R -factor is simply defined as: R_{OS} = fraction of energy range with experimental and theoretical slopes of opposite signs. Others are:

$$R_1 = A_1 \int |I_e - cI_t| dE,$$

$$R_2 = A_2 \int (I_e - cI_t)^2 dE,$$

$$\chi^2 = A_\chi \int (I_e - \bar{c}I_t)^2 dE,$$

with

$$c = \int I_e dE / \int I_t dE$$

(where c is beam-dependent, while \bar{c} is beam-averaged),

$$A_1 = 1 / \left(\int I_e dE \right),$$

$$A_2 = 1 / \left(\int I_e^2 dE \right),$$

$$A_\chi = 1 / \langle \int (I_e^2 - \bar{c}I_t)^2 dE \rangle.$$

Here the average (indicated by angled brackets) is taken over all available beams. Note that R_1 , R_2 and χ^2 can also be defined as finite sums over discrete energy points rather than as integrals, since they do not involve intensity derivatives. R_1 has been found to be quite reliable even when using large energy steps and to give about the same numbers as Pendry's R -factor [19]. R_1 has been denoted as R_{DE} in this context.

R_{P1} and R_{P2} are similar to R_1 and R_2 , but use the energy derivative I' of the intensity rather than the intensity I itself. The reduced Zanazzi–Jona R -factor additionally uses the second energy derivatives I'' :

$$R_{ZJ} = A_{ZJ} \int \frac{|I_e'' - cI_t''| |I_e' - cI_t'|}{(|I_e'| + \max |I_e''|)} dE,$$

with

$$A_{ZJ} = 1 / \left(0.027 \int I_e dE \right).$$

The Pendry R -factor uses a Y -function, which is a modification of the logarithmic derivative $L = I'/I$ of the intensity:

$$R_P = \frac{\int (Y_e - Y_t)^2 dE}{\int (Y_e^2 + Y_t^2) dE},$$

with

$$Y = L / (1 + V_{oi}^2 L^2).$$

In addition, a series of metrics has been defined by Philip and Rundgren [27,3]: these metrics compare the integral functions of the experimental and theoretical intensity curves.

These R -factors apply to I - V curves for individual beams; a weighted average over different beams gives the final R -factor for a particular structure. One may also use an average over different R -factors to combine their individual sensitivities to different features of I - V curves [3].

5.4.2. Using multiple R -factors

There is an advantage in simultaneously using more than one R -factor in a given study. It has been observed that in the near neighborhood of a global minimum (i.e. near a correct structure), all R -factors agree closely on the best-fit coordinates. By contrast, near local minima (i.e. near incorrect structures), the minimum locations of different R -factors deviate rather more from each other [74]. Thus, discrepancies between different R -factors can indicate an incorrect structure. Also, the scatter of the different best-fit coordinates corresponding to different R -factors will give a heuristic measure of the uncertainties associated with that structure.

As an example, one may compare R_p and R_2 applied to the case of Pt(111) and Pt(111)-(2 × 2)-O, with full relaxation down to the second metal layer: it is found that both R -factors give best-fit structures that agree within 0.01 Å for coordinates perpendicular to the surface. An incorrect structure (e.g. wrong adsorption site) gives structures that differ by as much as 0.1 Å from one R -factor to the other.

5.4.3. Clusters of R -factor minima

From the foregoing discussion, it appears that the appearance of clusters of shallow minima (for a single R -factor) is a signal of an incorrect structure: it may be sufficient to relax more atoms or coordinates (if one is near the global minimum), or it may be necessary to investigate a much different structure (if one is near a local minimum).

5.4.4. Avoiding fine-scale roughness of R -factors

When optimizing surface structures, it is important to have a smooth R -factor behavior, so that it does not exhibit fine noise or ripples in which a search algorithm can get trapped. Any R -factor can show fine-scale roughness, if the LEED calculations are not fully converged, if the integration is performed on too coarse an energy grid, or if edge truncation effects occur when the muffin-tin zero is varied.

For instance, R_p can be rough on a very short length scale (0.005 Å), when using an energy integration grid with 2 eV spacing. The logarithmic derivative used in R_p varies rapidly with energy at low-intensity points of an I - V curve, requiring a denser integration grid. To avoid the much higher computational costs due to a sufficiently fine energy grid, one may alternatively impose a uniform shift upward of both experimental and theoretical intensities by 5% of the average intensity, combined with a grid step of 0.25 eV. This smoothes R_p and solves the problem of numerical convergence. The automated search algorithms greatly benefit from this smoothing because more sophisticated and effective algorithms than the simplex method can be used effectively to locate the minimum. The smoothing accomplished by the shift also has the beneficial effect of eliminating spurious local minima which are inevitably associated with a rough R -factor hypersurface.

5.4.5. Sensitivity to experimental errors

Another critical issue is the sensitivity of different R -factors to experimental errors in the data. Ideally, one wants an R -factor which tolerates small systematic errors in the data, meaning that such errors raise the R -factor minimum but do not give rise to spurious or displaced minima corresponding to structural artifacts. If one has such an R -factor, then one can include the non-structural parameters in the structure search and be confident that the search algorithm will not drop into a spurious minimum.

An example of this is provided by considering the effect of an error in the angle of incidence, which, if unnoticed, leads to artificial lateral displacements of atoms in the surface.

By comparing model calculations for the Ni(100)-c(2 × 2)-O system, it has been shown [75] that an unknown error of a few tenths of a degree in the angle of incidence can lead to a best-fit, but purely artificial, asymmetric adsorption site in which the O atom is displaced laterally by 0.05 Å from the symmetric hollow site. (Note that such an error in lateral position will often fall within the error bars [76,77], in which case the uncertainty in angle of incidence is acceptable.)

Of the seven R -factors investigated, R_2 , R_{ZJ} , R_{p2} and R_{p1} tend to interpret this error as a spurious lateral displacement of the adsorbate. R_2 is particularly poor in this regard, the value at the artificial R -factor minimum being 18% below that of the symmetric site. Especially significant is the fact that the artificial minima are *correlated*: all four of these R -factors produce the same “best-fit” structure. In contrast, R_p , R_{OS} and R_1 do not produce such structural artifacts. These R -factors locate the correct best-fit structure, the angle of incidence leading only to a raising and broadening of the R -factor minimum. Thus R_p , R_{OS} and R_1 are quite stable with respect to small errors in the angle of incidence.

5.4.6. Theoretical energy steps

We next address the question of the optimal energy step used in the theory, with larger steps reducing the computational effort, while reducing the quality of interpolation. If one uses an integral R -factor (as opposed to one which does not rely on continuous curves and uses discrete summation), then one needs to calculate intensities on a grid which is dense enough compared to the typical peak width of $2V_{oi}$. Then higher-order polynomial interpolation can be used to whatever denser grid a given R -factor requires. The $2V_{oi}$ criterion implies that a grid step of about 3–5 eV is sufficient in most cases. This applies for the commonly used R -factors R_p , R_{ZJ} and metric distances.

Other R -factors, such as R_2 and R_1 , do not require the derivatives nor continuous I - V curves (they can be defined as sums over discrete energies rather than as integrals) and therefore allow a larger step width. In a detailed analysis [78] the effect of increasing the step width was investigated. It was found that R_1 and R_2 led to the same result, which agrees well with previous investigations [3]. A step width of up to 15–20 eV could be used without loss of precision. Further R -factors using \sqrt{I} rather than I (as for X-rays) have been studied as well, with no significantly different results. In general, R_1 (called R_{DE} in this case of discrete energies) was found to be the most reliable. Experience in a number of structural analyses has shown that the optimum step width depends on the number of beams and the energy range of the I - V curves. For short I - V curves, i.e. less than 100 eV, and a small number of beams, i.e. fewer than 8–10, it seems that a step width of 15 eV is too large, since the available database shrinks unacceptably. A step width of 5 eV is preferred in such a case.

In the nonlinear least-squares fit, R_2 rather than R_1 is minimized, because R_1 is not differentiable at the minimum. R_2 overestimates the misfit at strong peaks and the fit procedure always first tries to fit the prominent intensity maxima. It is therefore preferable to monitor the minimum of R_{DE} ($= R_1$), which is calculated simultaneously, while it is actually R_2 that is minimized.

5.4.7. Required number of R -factor evaluations

As a comment on the efficiency of search methods, we ask what is the smallest possible number of functional evaluations that will be needed to find a local minimum? To be certain that a minimum has been reached, one needs to at least explore its neighborhood enough to determine the shape of the R -factor hypersurface there. In the best possible scenario, in which there is only one minimum and the R -factor is well approximated by a simple quadratic

function of the coordinates, the number of parameters defining the quadratic form is approximately proportional to $N^2/2$, where N is the dimensionality of the parameter space, i.e. the number of parameters being fit. Therefore, at least of order $N^2/2$ functional evaluations will be needed to locate the minimum with certainty. (It is true that fewer evaluations may be sufficient to locate the minimum, but without providing certainty that it is really a minimum.) Quite generally, we empirically find that this number scales like cN^2 , where c is a constant of order 10. In practical terms, using a concrete example: given a time on the order of a second or less for a single R -factor evaluation using TLEED for a particular structure on an IBM RISC 320E workstation, searches in which 30 to 40 parameters are relaxed simultaneously are readily feasible; on a supercomputer, 100 parameters could be fit today with a few hours of CPU time.

5.5. Optimization strategies

5.5.1. Optimizing subsets of parameters

In LEED optimization, the R -factor generally will depend more strongly on some parameters than on others. For instance, LEED R -factors vary more rapidly with changes in coordinates perpendicular to the surface than in those parallel to the surface (because of the usual near-normal momentum transfer), and depend more on coordinates near the surface than deep below the surface (because of the damping). Thus we divide parameters into sensitive – those that have a strong influence on intensities – and insensitive – those that only weakly influence intensities.

Due to the finite mean free path in LEED, one must limit the fitting of coordinates to atoms near the surface. It is useless to try fitting coordinates of atoms deeper than twice the mean free path ($\sim 10 \text{ \AA}$): otherwise deep atoms will artificially move by large amounts to compensate for any deficiencies in theory or experiment.

If one allows all parameters to vary at the same time, especially in initial stages of a search, any error in the guess of sensitive parameters can cause wild initial changes in the insensitive parameters. These changes must then be largely reversed in later stages of the search, slowing down the search considerably. Generally, these insensitive parameters can be recognized by the large error bars associated with them (see section 5.6).

Experience in X-ray crystallography has shown that it is often more efficient to first optimize sensitive parameters, while keeping insensitive parameters fixed. Applied to LEED, this means first fitting coordinates perpendicular to the surface (together with the muffin-tin zero), then in addition coordinates parallel to the surface, and finally (if desired) fitting all coordinates and various non-structural parameters at the same time.

An additional option is to relax the surface symmetry in gradual steps. One might start with a guessed initial structure that has the highest symmetry compatible with the substrate symmetry and the observations (e.g. high-symmetry adsorption site), and restrict the search at first to structures which maintain that symmetry. In subsequent optimizations, the symmetry constraints could be gradually lifted.

Here caution must be exercised with equivalent domains of different orientation, called twinning in the three-dimensional bulk case: one should average over such domains; this also maintains compatibility with diffraction patterns that exhibit higher symmetry than the trial structures have. It is important to realize that in X-ray crystallography, the structural analysis is often seriously hindered by twinning of the crystal, the equivalent of surface domains.

An advantage of gradual symmetry breaking is that the dimensionality of the parameter space is kept to a minimum, thus allowing a more effective and faster search. A danger,

however, is that one could get trapped in a local minimum. One must in particular make sure that the chosen search algorithm actually explores lower-symmetry structures: methods like least-squares fit and steepest descent will not break the symmetry of the initial structure; for these one must therefore provide an asymmetrical initial structure to start with.

Given real data and allowing the search to explore low-symmetry structures, the optimum structure will in fact most likely exhibit no symmetry at all. Even when the actual structure is in fact symmetrical, the fitting process will break that symmetry to some extent because of experimental noise and because of imperfect convergences in the calculation. It is then impossible to tell whether the actual structure in fact retains any symmetry: one's knowledge is limited by the error bars. It may be tempting to accept a lower-symmetry model that gives a better fit (thanks to its additional parameters) than a higher-symmetry model, but one has to accept that the symmetry breaking may be due to imperfections in theory or experiment.

5.5.2. Iterating the search

It is advisable to iterate any search process at least once; a completely fresh search (including a new dynamical LEED calculation as needed) should be started from the best structure found in the last search. This is clearly necessary when the best structure deviates from the initial guess by a distance comparable to the convergence radius of the approximation (e.g. 0.2 Å in the case of TLEED).

The situation will also arise in which a search runs away from the initial guess towards a relatively distant minimum. If the search reaches too far for the approximation to be reliable, it is necessary to restart the procedure at the last point reached. This may have to be iterated more than once, depending on the distance to the nearest minimum. However, this situation has not yet occurred in our experience.

5.5.3. Checking for a minimum

With an optimization algorithm, it is valuable to be able to explicitly check that the search has indeed found a minimum, rather than a saddle point, say. A very convenient method is simply to plot the R -factor along the set of all the principal directions (i.e. not necessarily the Cartesian or other physical coordinates): if and only if we have located a local minimum will all these curves show a minimum at the best-fit positions.

To improve confidence it also helps to restart the search from different initial positions in the neighborhood of the minimum found and to check that the same best-fit structure is obtained in each case. However, there is no avoiding the dangers of local minima distant from the desired global minimum. It is also impossible to guarantee that a given minimum is the global minimum and not a local minimum. The more extensive the search (through assuming a variety of initial trial structures), the higher the confidence in the result.

It is helpful that local minima are often (but not always) characterized by unphysical bond lengths and bond angles: as in X-ray crystallography, this is a powerful criterion. Such a criterion has so far not been formalized as a "penalty function" in LEED R -factors, but could easily be built in. This assumes knowledge of certain structural preferences for surfaces, which are emerging from the hundreds of surface structures determined to date.

5.6. Structural precision and accuracy

5.6.1. Accuracy poorly known

Structural uncertainties arise from random errors (corresponding to precision) and systematic errors (corresponding to accuracy). As mentioned in section 2 for the case of X-ray

crystallography, systematic errors are very difficult to estimate: this holds true at least as strongly in the case of LEED. And since the systematic errors in XRD often lead to error bars which are an order of magnitude larger than do the random errors, one should expect the same in LEED. For this reason, a *statistical* analysis of error bars in LEED is in principle not very meaningful. As a result, there is, unfortunately, no agreed upon scheme for determining error bars in LEED crystallography.

It is useful to realize that in X-ray diffraction the same discussion about systematic errors and model assumptions has been carried on for a long time [79].

5.6.2. Estimating error bars

Nonetheless, several relatively objective schemes have been proposed within LEED to determine the *statistical* error bars, i.e. precision. They yield reasonable error-bar values in part because they make certain independent assumptions about the number of data points used. Specifically, it is not the total number of measured intensities that is counted, but rather the number of peaks in I - V curves.

Among these schemes, we mention Pendry's RR -factor which measures the reliability of the R -factor [80], and Adams' standard deviations [81]. In addition, one may use the scatter in best-fit coordinates due to different R -factors or different subsets of the database as a heuristic measure of the error bars [74].

5.6.3. Correlated parameters

Error bars are only well defined for the principal directions discussed previously, rather than for the initial Cartesian coordinates. This is because of correlations between parameters: in Cartesian coordinates, one would obtain a full error matrix with off-diagonal terms due to these correlations [81]. Only in the case of uncorrelated parameters do the principal directions and associated error bars coincide with the Cartesian coordinates and does one get a diagonal error matrix, i.e. independent uncertainties in the individual Cartesian coordinates.

Once diagonalized, the error matrix does provide meaningful information, namely error bars on certain linear combinations of the parameters: unfortunately, it is not very useful to tabulate these linear combinations. Error matrices are also too cumbersome and uninformative to publish. As a result, the custom in X-ray crystallography is to ignore off-diagonal terms of the error matrix and publish the diagonal terms of the undiagonalized matrix, as if there were no correlations (a full discussion of this issue can be found in the literature [28]). The same practice can therefore also be adopted in LEED crystallography.

5.6.4. Error bar definitions

In both Adams' and Pendry's approaches, the error bar corresponding to a certain coordinate is given by the curvature $1/\epsilon$ of the R -factor at the minimum measured along that coordinate, by the minimum R -factor value R_0 itself, as well as by the number of independent data points available:

$$\begin{aligned}\sigma_A^2 &= \epsilon R_0 / N, \\ \sigma_P^2 &= \epsilon R_0 / \sqrt{N/8}.\end{aligned}$$

While Adams takes for N the number of kinematic Bragg peaks contained within the energy range of the measurements ΔE , Pendry estimates the number of peaks including multiple scattering effects and takes $N = \Delta E / 4 |V_{oi}|$, where V_{oi} is the imaginary part of the inner potential [82,80].

Generally speaking, because of different assumptions, the Adams error bar tends to be optimistic, and the Pendry error bar conservative for the same structure determination; a factor of 3 between them is typical, but not systematic.

5.6.5. Examples

It is not surprising to find in practice that the error bars become larger for atoms that are deeper in the solid (due to damping) and for coordinates parallel to the surface (due to the momentum transfer having its largest component perpendicular to the surface). For example, buckling in the topmost metal layer of Pt(111)-(2 × 2)-O causes a drop in Pendry R -factor from 0.267 to 0.193; the Pendry error bar on the optimal buckling of 0.08 Å is 0.04 Å, making the buckling significant. By contrast, the inclusion of lateral relaxation in the same Pt layer causes a small further drop of the R -factor to 0.176, while the corresponding error bars (0.04 Å) are larger than the measured lateral displacement from the bulk position (0.03 Å), rendering it possibly insignificant. However, the significant buckling is a robust property: it is not sensitive to using a different R -factor, a different energy range, or for example integer or fractional beams.

It is also of interest to compare the error bars on various non-structural parameters. This was discussed in section 5.1 under the heading: Relative importance of non-structural parameters.

6. Application to other spectroscopies

Besides LEED, a number of other techniques are used to determine surface structures. With those techniques which are based on electron scattering, it is in principle possible to automate the process with the same methods described here for LEED. This is especially true of techniques like photoelectron diffraction (PED) [83], Auger electron diffraction (AED) [83], high-resolution electron energy-loss spectroscopy (HREELS) [84] and near-edge X-ray absorption fine structure (NEXAFS) [85]. All of these involve multiple-scattering effects for which the methods developed for LEED are perfectly suitable. In fact, these techniques already utilize computational methods derived in large part from or similar to conventional LEED theory.

As an example, the TLEED formalism can be applied quite straightforwardly to photoelectron diffraction and then combined with an automated search scheme. The TLEED formalism, thanks to its flexibility, does not depend on the electron source being a plane wave, or on the surface being periodic: point-source emission can easily be accommodated, as can disordered layers.

7. Conclusions and outlook

The recent developments in LEED theory have pushed the technique very close to the level of automation of surface-structure determination known in X-ray crystallography. This has been accomplished both by introducing more efficient methods for computing LEED intensities, and by using search algorithms that allow many structural (and non-structural) parameters to be determined. This development is of great importance: it will soon be possible to perform LEED crystallography without the need for a theoretician, a great

advantage, by using “black-box” LEED programs similar to those available in X-ray crystallography. However, improvements are still needed, including:

- expert dynamical LEED programs that organize themselves to most efficiently handle more complex surface geometries, e.g. programs that automatically decide which layers to combine within the spherical-wave representation rather than the plane-wave representation (in the combined-space method), and that automatically choose among such schemes as layer doubling and renormalized forward scattering;
- automated treatment of symmetries;
- better treatment of atomic scattering potentials, thermal vibrations and defects;
- user-friendliness of programs.

Automatic refinement has already allowed far more complex surface structures to be solved than before. This capability also permits higher-accuracy determinations, perhaps on the picometer scale of 0.01 Å. It may be possible to achieve even higher accuracy: this is found in X-ray crystallography to require anisotropic vibrations. The same improvement is a clear possibility in LEED (despite the added complication of correlations in vibrations of nearby atoms, sensed through multiple scattering). But other non-structural parameters probably will need to be improved. For instance, it may become necessary to use non-spherical scattering potentials, which may add considerably to the computational cost. It is nevertheless possible that such non-structural parameters could be routinely fit to experiment in the same process as the structure determination.

Badly lacking in LEED is an analogue of the direct method of X-ray crystallography for directly determining a structure without a trial-and-error search, or even a method (analogous to the Patterson transform) to produce a rough model of the structure.

Finally, the automated methods developed for LEED can easily be adapted to other electron-based techniques, like photoelectron and Auger electron diffraction, high-resolution electron energy-loss spectroscopy and near-edge X-ray absorption fine structure.

Acknowledgments

We are grateful for helpful discussions with K. Heinz and D.L. Adams. This work was supported in part by the Director, Office of Energy Research, Office of Basic Energy Sciences, Materials Sciences Division, of the US Department of Energy under contract number DE-AC03-76SF00098. Supercomputer time was provided by the US Department of Energy, and by the University of California at Berkeley. A.W. gratefully acknowledges support from NATO via the SERC UK. P.J.R. gratefully acknowledges support from the Digital Equipment Corporation through the Science Innovators Program. U.S. gratefully acknowledges support by the Deutsche Forschungsgemeinschaft (DFG).

References

- [1] J.B. Pendry, *Low Energy Electron Diffraction* (Academic Press, New York, 1974).
- [2] M.A. Van Hove and S.Y. Tong, *Surface Crystallography by LEED* (Springer, Berlin, 1979).
- [3] M.A. Van Hove, W.H. Weinberg and C.M. Chan, *Low-Energy Electron Diffraction* (Springer, Berlin, 1986).
- [4] M.A. Van Hove, in: *Chemistry and Physics of Solid Surfaces VII*, Eds. R.F. Howe and R. Vanselow (Springer, Berlin, 1988) p. 513.
- [5] K. Heinz, *Prog. Surf. Sci.* 27 (1988) 239.

- [6] R.S. Zimmer and B.W. Holland, *J. Phys. C* 8 (1975) 2395.
- [7] D. Aberdam, R. Baudoing and C. Gaubert, *Surf. Sci.* 52 (1975) 125.
- [8] S.Y. Tong, M.A. Van Hove and B.J. Mrstik, in: *Proc. 7th IVC/3rd ICSS, Vienna, 1977*, Eds. R. Dobrozemsky, F. Rüdener and F.P. Viehböck, p. 2407.
- [9] K. Heinz and G. Besold, *Surf. Sci.* 125 (1983) 515.
- [10] M.A. Van Hove, R.F. Lin and G.A. Somorjai, *Phys. Rev. Lett.* 51 (1983) 778.
- [11] J. Rundgren and A. Salwén, *Comput. Phys. Commun.* 9 (1975) 312.
- [12] W. Moritz and D. Wolf, *Surf. Sci.* 163 (1985) L655.
- [13] S.Y. Tong, H. Huang, C.M. Wei, W.F. Packard, F.K. Men, G. Glander and M.B. Webb, *J. Vac. Sci. Technol. A* 6 (1988) 615.
- [14] D.L. Adams, in: *Proc. 1st Int. Seminar on Surface Structure Determination by LEED, Erlangen, 1985* (unpublished), p. 28.
- [15] G.H. Stout and L.H. Jensen, *X-Ray Structure Determination* (MacMillan, New York, 1968).
- [16] P.G. Cowell and V.E. de Carvalho, *Surf. Sci.* 187 (1987) 175.
- [17] P.J. Rous and J.B. Pendry, in: *The Structure of Surfaces II*, Eds. J.F. van der Veen and M.A. Van Hove (Springer, Berlin, 1988) p. 14.
- [18] P.J. Rous, M.A. Van Hove and G.A. Somorjai, *Surf. Sci.* 226 (1990) 15.
- [19] G. Kleinle, W. Moritz, D.L. Adams and G. Ertl, *Surf. Sci.* 219 (1989) L637.
- [20] G. Kleinle, W. Moritz and G. Ertl, *Surf. Sci.* 238 (1990) 119.
- [21] P.J. Rous, *Prog. Surf. Sci.* 39 (1992) 3.
- [22] A. Wander, A. Barbieri, U. Starke, N. Materer, M.A. Van Hove and G.A. Somorjai, in preparation.
- [23] D.W. Jepsen, *Phys. Rev. B* 22 (1980) 5701.
- [24] P. Pinkava and S. Crampin, *Surf. Sci.* 223 (1990) 27.
- [25] X.-G. Zhang, P.J. Rous, J.M. MacLaren, A. Gonis, M.A. Van Hove and G.A. Somorjai, *Surf. Sci.* 239 (1990) 103.
- [26] X.-G. Zhang, M.A. Van Hove, G.A. Somorjai, P.J. Rous, D. Tobin, A. Gonis, J.M. MacLaren, K. Heinz, M. Michl, H. Lindner, K. Müller, M. Ehsasi and J.H. Block, *Phys. Rev. Lett.* 67 (1991) 1298.
- [27] J. Philip and J. Rundgren, in: *Determination of Surface Structure by LEED*, Eds. P.M. Marcus and F. Jona (Plenum, New York, 1981) p. 425.
- [28] J.D. Dunitz, *X-Ray Analysis and The Structure of Organic Molecules* (Cornell University Press, Ithaca, NY, 1979);
see also, for a detailed discussion of error estimates and precision: E. Prince, *Mathematical Techniques in Crystallography and Materials Science* (Springer, Heidelberg, 1982).
- [29] P.J. Rous, J.B. Pendry, D.K. Saldin, K. Heinz, K. Müller and N. Bickel, *Phys. Rev. Lett.* 57 (1986) 2951.
- [30] P.J. Rous and J.B. Pendry, *Comput. Phys. Commun.* 54 (1989) 137.
- [31] P.J. Rous and J.B. Pendry, *Comput. Phys. Commun.* 54 (1989) 157.
- [32] P.J. Rous and J.B. Pendry, *Surf. Sci.* 219 (1989) 355, 373.
- [33] P.J. Rous, D. Jentz, D.G. Kelly, R.Q. Hwang, M.A. Van Hove and G.A. Somorjai, in: *The Structure of Surfaces III*, Eds. S.Y. Tong, M.A. Van Hove, K. Takayanagi and X.D. Xie (Springer, Berlin, 1991) p. 432.
- [34] J. Dunphy, Ph. Sautet, M. Salmeron, D. Jentz, A. Barbieri, M.A. Van Hove and G.A. Somorjai, to be published.
- [35] A. Wander, M.A. Van Hove and G.A. Somorjai, *Phys. Rev. Lett.* 67 (1991) 626.
- [36] U. Starke, A. Barbieri, N. Materer, M.A. Van Hove and G.A. Somorjai, *Surf. Sci.* 286 (1993) 1.
- [37] U. Starke, N. Materer, R. Döll, M. Michl, K. Heinz, A. Barbieri, M.A. Van Hove and G.A. Somorjai, *Surf. Sci.* 287 (1993) 432.
- [38] D. Jentz, A. Barbieri, G. Held, M.A. Van Hove, J. Dunphy, Ph. Sautet, M. Salmeron and G.A. Somorjai, to be published.
- [39] J.M. Powers, A. Wander, P.J. Rous, M.A. Van Hove and G.A. Somorjai, *Phys. Rev. B* 44 (1991) 11 159.
- [40] J.M. Powers, A. Wander, M.A. Van Hove and G.A. Somorjai, *Surf. Sci. Lett.* 260 (1992) L7.
- [41] H. Over, U. Ketterl, W. Moritz and G. Ertl, *Phys. Rev. B* 46 (1992) 15 438.
- [42] R. Baudoing-Savois, Y. Gauthier and W. Moritz, *Phys. Rev. B* 44 (1991) 12 977.
- [43] H. Over, G. Kleinle, G. Ertl, W. Moritz, K.-H. Ernst, H. Wohlgenuth, K. Christmann and E. Schwarz, *Surf. Sci. Lett.* 254 (1991) L469.
- [44] H. Over, H. Bludau, M. Skottke-Klein, G. Ertl, W. Moritz and C.T. Campbell, *Phys. Rev. B* 45 (1992) 8638.
- [45] R. Zuschke, Zi Pu Hu, D. Wolf, W. Moritz, N. Fischer, P. Dürr and Th. Fauster, to be published.
- [46] H. Over, H. Bludau, M. Skottke-Klein, W. Moritz and G. Ertl, *Phys. Rev. B* 46 (1992) 4360.
- [47] C. Stampfl, M. Scheffler, H. Over, J. Burchhardt, M. Nielsen, D.L. Adams and W. Moritz, *Phys. Rev. Lett.* 69 (1992) 1532.
- [48] R. Zuschke, W. Moritz and D. Wolf, *Surf. Sci.*, to be published.

- [49] T. Grünberg, B. Vogler, W. Moritz and D. Wolf, to be published.
- [50] A. Wander, J.B. Pendry and M.A. Van Hove, *Phys. Rev. B* 46 (1992) 9897.
- [51] J.B. Pendry, *Surf. Sci. Rep.* 19 (1993) 87.
- [52] A. Wander, L.D. Mapledoram, C.J. Barnes and D.A. King, in preparation.
- [53] W.H. Press, B.P. Flannery, S.A. Teukolsky and W.T. Vetterling, *Numerical Recipes* (Cambridge University Press, Cambridge, 1986).
- [54] K. Heinz, W. Oed and J.B. Pendry, *Phys. Rev. B* 41 (1990) 10179.
- [55] D.W. Marquardt, *J. Soc. Ind. Appl. Math.* 11 (1963) 431.
- [56] H.H. Rosenbrock, *Comput. J.* 3 (1960) 175.
- [57] R.P. Brent, *Numerical Recipes: Algorithms for Minimization without Derivatives* (Prentice-Hall, Englewood Cliffs, NJ, 1973).
- [58] M.M. Woolfson, *An Introduction to X-Ray Crystallography* (Cambridge University Press, Cambridge, 1979).
- [59] D.L. Adams, U. Landman and J.C. Hamilton, *J. Vac. Sci. Technol.* 12 (1974) 260.
- [60] J.B. Pendry, K. Heinz and W. Oed, *Phys. Rev. Lett.* 61 (1988) 2953.
- [61] J.B. Pendry and K. Heinz, *Surf. Sci.* 230 (1990) 137.
- [62] J.B. Pendry, K. Heinz and W. Oed, *Vacuum* 41 (1990) 340.
- [63] K. Heinz, W. Oed and J.B. Pendry, in: *The Structure of Surfaces III*, Eds. S.Y. Tong, M.A. Van Hove, K. Takayanagi and X.D. Xie (Springer, Heidelberg, 1991) p. 139.
- [64] W. Oed, P.J. Rous and J.B. Pendry, *Surf. Sci.* 273 (1992) 261.
- [65] J.B. Pendry, *Phil. Trans. R. Soc.* 334 (1991) 539.
- [66] J.B. Pendry, *J. Phys. C* 13 (1980) 937.
- [67] M. Maglietta, *Solid State Commun.* 43 (1982) 395.
- [68] W. Kohn and N. Rostocker, *Phys. Rev.* 94 (1954) 1111.
- [69] J. Koringa, *Physica* 13 (1947) 392.
- [70] R.P. Messmer, in: *The Nature of The Surface Chemical Bond*, Eds. T.N. Rhodin and G. Ertl (North-Holland, Amsterdam, 1979) p. 51.
- [71] D.L. Adams, H.B. Nielsen and M.A. Van Hove, *Phys. Rev. B* 20 (1979) 4789.
- [72] P. de Andres, P.J. Rous and J.B. Pendry, *Surf. Sci.* 191 (1988) 1.
- [73] K. Heinz, U. Starke, M.A. Van Hove and G.A. Somorjai, *Surf. Sci.* 261 (1992) 57.
- [74] An extensive account of many different *R*-factors and their use in LEED is given in: M.A. Van Hove and R.J. Koestner, in: *Determination of Surface Structure by LEED*, Eds. P.M. Marcus and F. Jona (Plenum, New York, 1984) p. 357.
- [75] P.J. Rous, unpublished.
- [76] W. Oed, H. Lindner, U. Starke, K. Heinz, K. Müller and J.B. Pendry, *Surf. Sci.* 224 (1989) 179.
- [77] D. von Gemünden, PhD Thesis, University of Erlangen (1990).
- [78] G. Kleinle, W. Moritz, D.L. Adams and G. Ertl, *Surf. Sci.* 219 (1989) L637; G. Kleinle, PhD Thesis, Free University of Berlin (1990).
- [79] D. Schwarzenbach, S.C. Abrahams, H.D. Flack, W. Gonschorek, Th. Hahn, K. Huml, R.E. Marsh, E. Prince, B.E. Robertson, J.S. Rollett and A.J.C. Wilson, *Acta Cryst. A* 45 (1989) 63.
- [80] J.B. Pendry, *J. Phys. C* 13 (1980) 937.
- [81] H.B. Nielsen and D.L. Adams, *J. Phys. C* 15 (1982) 615.
- [82] D.L. Adams, V. Jensen, X.F. Sun and J.H. Vollesen, *Phys. Rev. B* 38 (1988) 7913.
- [83] C.S. Fadley, *Phys. Scr.* T17 (1990) 39.
- [84] Z.Q. Wu, M.L. Xu, Y. Chen, S.Y. Tong, M.H. Mohamed and L.L. Kesmodel, *Phys. Rev. B* 36 (1987) 9329.
- [85] J. Stöhr, *NEXAFS Spectroscopy* (Springer, Berlin, 1992).